

ROBUST A POSTERIORI ERROR ANALYSIS FOR ROTATION-BASED FORMULATIONS OF THE ELASTICITY/POROELASTICITY COUPLING*

VERÓNICA ANAYA[†], ARBAZ KHAN[‡], DAVID MORA[†], AND RICARDO RUIZ-BAIER[§]

Abstract. We develop the a posteriori error analysis of three mixed finite element formulations for rotation-based equations in elasticity, poroelasticity, and interfacial elasticity-poroelasticity. The discretizations use H^1 -conforming finite elements of degree $k+1$ for displacement and fluid pressure, and discontinuous piecewise polynomials of degree k for rotation vector, total pressure, and elastic pressure. Residual-based estimators are constructed, and upper and lower bounds (up to data oscillations) for all global estimators are rigorously derived. The methods are all robust with respect to the model parameters (in particular, the Lamé constants); they are valid in 2D and 3D, and also for arbitrary polynomial degree $k \geq 0$. The error behavior predicted by the theoretical analysis is then demonstrated numerically on a set of computational examples including different geometries on which we perform adaptive mesh refinement guided by the a posteriori error estimators.

Key words. mixed finite element method, linear poroelasticity, rotation-based formulations, interface problems, a priori and a posteriori error estimation

MSC codes. 65N30, 65N50, 74F99, 74A50, 76S05

DOI. 10.1137/21M1427516

1. Introduction. The interaction between interstitial fluid flow and the deformation of the underlying porous structure gives rise to a variety of mechanisms of fluid-structure coupling. In the specific case of Biot poromechanics, this interaction occurs when the linearly elastic porous medium is saturated, and such a problem is relevant to a large class of very diverse applications ranging from bone healing to, e.g., petroleum engineering or sound isolation. We are also interested in the interface between elastic and poroelastic systems that is encountered in hydrocarbon production in deep subsurface reservoirs (a pay zone and the surrounding nonpay rock formation) [24], or in the study of tooth and periodontal ligament interactions [4].

Rotation-based formulations are found in applications to the modelling of nonporous media and helicoidal motion (see, e.g., [7, 29, 34] and the references therein). The

*Submitted to the journal's Computational Methods in Science and Engineering section June 17, 2021; accepted for publication (in revised form) April 7, 2022; published electronically August 4, 2022.

<https://doi.org/10.1137/21M1427516>

Funding: This work was partially supported by DIUBB through projects 2020127 IF/R and 2120173 GI/C, by ANID-Chile through projects FONDECYT 1211265 and ACE210010, Centro de Modelamiento Matemático (FB210005), by the Sponsored Research & Industrial Consultancy (SRIC), Indian Institute of Technology Roorkee, India through the faculty initiation grant MTD/FIG/100878, by SERB MATRICS grant TR/2020/000303, by the Monash Mathematics Research Fund S05802-3951284, and by the Ministry of Science and Higher Education of the Russian Federation within the framework of state support for the creation and development of World-Class Research Centers “Digital Biodesign and Personalised Healthcare” 075-15-2020-926.

[†]GIMNAP, Departamento de Matemática, Universidad del Bío-Bío, Concepción, 4051381, Chile, and CI²MA, Universidad de Concepción, Concepción, Chile 4070386 (vanaya@ubiobio.cl, dmora@ubiobio.cl).

[‡]Department of Mathematics, Indian Institute of Technology Roorkee, Roorkee 247667, India (arbaz@ma.iitr.ac.in).

[§]School of Mathematics, Monash University, 9 Rainforest Walk, Melbourne 3800 VIC, Australia; World-Class Research Center “Digital Biodesign and Personalized Healthcare”, Sechenov First Moscow State University, Moscow, Russia, 119435; and Universidad Adventista de Chile, Casilla 7-D, Chillán, 3780000, Chile (ricardo.ruizbaier@monash.edu).

resulting theory has a similarity with vorticity-based formulations for incompressible flow such as [6, 11, 19, 21, 27].

The schemes for elasticity and transmission elasticity-poroelasticity and their a priori error analysis have been studied in [5] and [4], respectively. The solvability of the rotation-based poroelasticity has not been addressed yet, and for sake of completeness we outline its analysis in Appendices A and B. The well-posedness of the continuous problem is studied by grouping the unknowns with compatible regularity and realizing that the resulting problem is a mixed variational formulation that resembles the system introduced in [32, 37] that describes the Biot equations in their displacement-pressure-total pressure formulation. Our analysis also discusses the limit case when the specific storage coefficient goes to zero, and we observe that the continuous dependence on data is robust with respect to the Lamé constants.

Our focus is on the design, analysis, and testing of a posteriori error estimators for these three rotation-based models and discretizations. Robust a posteriori error estimators for Biot poroelasticity are relatively recent in the literature. They include a reliable estimator based on stress and flux reconstructions [38], the weakly symmetric tensor reconstruction for total stress and Darcy flux from [12, 24], a reliable space-time a posteriori error estimator for a four-field system from [1] (requiring the solution of auxiliary local problems), the guaranteed equilibrated bounds for fixed-stress splitting scheme from [31] and for double-diffusive poroelasticity from [35] and for multiple network poroelasticity recently advanced in [20], the robust residual a posteriori estimates for displacement-flux-pressure advanced in [33], and for displacement-elastic pressure-fluid pressure from [30, 36]. We follow the latter approaches and construct residual-type error estimators. All of the terms that conform the a posteriori error estimators are easily fully computable locally. The derivation of the upper bounds for each of the terms conforming the a posteriori estimators for rotation-based elasticity and rotation-based poroelasticity is based on exploiting scaling arguments and bubble function techniques. The results obtained for these two subproblems are then combined with estimates for the additional terms that appear in the transmission problem. As mentioned above, in all cases a careful treatment of the model parameters is essential to maintain robustness with respect to the sensible Lamé constants of the elastic and poroelastic media (going to infinity when the Poisson ratio approaches 1/2).

The remainder of this paper has been structured in the following manner. Instead of grouping the continuous results together and the error bounds separately for all problems, we have divided the analysis by type of problem. Therefore, section 2 defines the rotation-based elasticity problem, recalls the solvability and stability of the continuous problem and of the mixed finite element discretization, and provides the construction and analysis of an a posteriori error estimator. An analogous presentation is given in section 3 for the rotation-based Biot equations. These results are then combined in section 4 to treat the rotation-based transmission problem between a poroelastic and an elastic subdomain. A few examples are presented in section 5, showing, in particular, that mesh adaptivity steered by the a posteriori error estimators leads to an important reduction in the number of degrees of freedom that are needed to reach a certain accuracy level, and the tests also indicate the sharpness of the a posteriori error analysis. We also illustrate the use of the adaptive method in the simulation of a three-dimensional aquifer interface problem. Finally, in Appendices A and B, we present the a priori error analysis of the rotation-based poroelasticity problem. Some concluding remarks and possible extensions are collected in section 6.

2. Rotation-based linear elasticity. This section is devoted to deriving reliability and efficiency of a residual a posteriori error estimator for a formulation of linear elasticity in terms of rotation, displacement, and pressure. We start with preliminary results regarding the continuous and discrete formulations.

2.1. Continuous formulation. Let $\Omega \subset \mathbb{R}^d$, $d \in \{2, 3\}$, be a bounded Lipschitz domain with boundary $\Gamma := \partial\Omega$. Our starting point is the rotation-based elasticity problem, as proposed in [5]: Given an external force \mathbf{f}^E , we seek the displacement \mathbf{u} , the rotation $\boldsymbol{\omega}$, and the pressure p such that

$$(2.1a) \quad \sqrt{\mu^E} \operatorname{curl} \boldsymbol{\omega} + \nabla p = \mathbf{f}^E \quad \text{in } \Omega,$$

$$(2.1b) \quad \boldsymbol{\omega} - \sqrt{\mu^E} \operatorname{curl} \mathbf{u} = 0 \quad \text{in } \Omega,$$

$$(2.1c) \quad \operatorname{div} \mathbf{u} + (2\mu^E + \lambda^E)^{-1} p = 0 \quad \text{in } \Omega,$$

$$(2.1d) \quad \mathbf{u} = \mathbf{0} \quad \text{on } \Gamma,$$

where μ^E and λ^E are the Lamé coefficients (material properties of the solid, and here assumed constant). The weak formulation of (2.1) is as follows: find $(\mathbf{u}, \boldsymbol{\omega}, p) \in \mathbf{H}_0^1(\Omega) \times \mathbf{L}^2(\Omega) \times L^2(\Omega)$ such that

$$(2.2a) \quad -\sqrt{\mu^E} \int_{\Omega} \operatorname{curl} \mathbf{v} \cdot \boldsymbol{\omega} + \int_{\Omega} p \operatorname{div} \mathbf{v} = - \int_{\Omega} \mathbf{f}^E \cdot \mathbf{v} \quad \forall \mathbf{v} \in \mathbf{H}_0^1(\Omega),$$

$$(2.2b) \quad \int_{\Omega} \boldsymbol{\omega} \cdot \boldsymbol{\theta} - \sqrt{\mu^E} \int_{\Omega} \boldsymbol{\theta} \cdot \operatorname{curl} \mathbf{u} = 0 \quad \forall \boldsymbol{\theta} \in \mathbf{L}^2(\Omega),$$

$$(2.2c) \quad \int_{\Omega} \operatorname{div} \mathbf{u} q + (2\mu^E + \lambda^E)^{-1} \int_{\Omega} pq = 0 \quad \forall q \in L^2(\Omega),$$

or more conveniently written in the form

$$B_E((\mathbf{u}, \boldsymbol{\omega}, p), (\mathbf{v}, \boldsymbol{\theta}, q)) = -(\mathbf{f}^E, \mathbf{v})_{0,\Omega},$$

where the multilinear form (having a subscript E, for *elasticity*) is

$$\begin{aligned} B_E((\mathbf{u}, \boldsymbol{\omega}, p), (\mathbf{v}, \boldsymbol{\theta}, q)) := & -\sqrt{\mu^E} \int_{\Omega} \operatorname{curl} \mathbf{v} \cdot \boldsymbol{\omega} + \int_{\Omega} p \operatorname{div} \mathbf{v} + \int_{\Omega} \boldsymbol{\omega} \cdot \boldsymbol{\theta} \\ & - \sqrt{\mu^E} \int_{\Omega} \boldsymbol{\theta} \cdot \operatorname{curl} \mathbf{u} + \int_{\Omega} \operatorname{div} \mathbf{u} q + (2\mu^E + \lambda^E)^{-1} \int_{\Omega} pq. \end{aligned}$$

For the considered boundary conditions, the term $\operatorname{div} \mathbf{H}_0^1(\Omega)$ can control only the L^2 norm of the mean-value zero part of p , and an additional contribution is needed to control the mean-value part of p (see, e.g., [32]). Thus we can decompose p into P_{mp} and $p_0 = p - P_{mp}$, where P_{mp} is the mean value part and p_0 is the mean value zero part. This is required only in the incompressibility limit, as Herrmann's problem approaches Stokes equations and pressure (for \mathbf{u} prescribed everywhere on the boundary) is no longer unique. This will be relevant also in the case of rotation-based Biot equations discussed in section 3, below.

The well-posedness of the above variational problem is a direct consequence of the following result (see [23]).

THEOREM 2.1. *For every $(\mathbf{u}, \boldsymbol{\omega}, p) \in \mathbf{H}_0^1(\Omega) \times \mathbf{L}^2(\Omega) \times L^2(\Omega)$, there exists $(\mathbf{v}, \boldsymbol{\theta}, q) \in \mathbf{H}_0^1(\Omega) \times \mathbf{L}^2(\Omega) \times L^2(\Omega)$ with $\|(\mathbf{v}, \boldsymbol{\theta}, q)\| \leq C_1 \|(\mathbf{u}, \boldsymbol{\omega}, p)\|$ such that*

$$B_E((\mathbf{u}, \boldsymbol{\omega}, p), (\mathbf{v}, \boldsymbol{\theta}, q)) \geq C_2 \|(\mathbf{u}, \boldsymbol{\omega}, p)\|^2,$$

where $\|(\mathbf{v}, \boldsymbol{\theta}, q)\|^2 := \mu^E \|\mathbf{curl} \mathbf{v}\|_{0,\Omega}^2 + \mu^E \|\operatorname{div} \mathbf{v}\|_{0,\Omega}^2 + \|\boldsymbol{\theta}\|_{0,\Omega}^2 + (2\mu^E + \lambda^E)^{-1} \|q\|_{0,\Omega}^2 + (\mu^E)^{-1} \|q_0\|_{0,\Omega}^2$.

Proof. Consider the decomposition $p = p_0 + P_m p$. As a consequence of the inf-sup condition, for every $p_0 \in L_0^2(\Omega)$ there exists $\mathbf{v}_0 \in \mathbf{H}_0^1(\Omega)$ such that $(p_0, \operatorname{div} \mathbf{v}_0)_{0,\Omega} \geq C_\Omega (\mu^E)^{-1} \|p_0\|_{0,\Omega}^2$ and $(\mu^E)^{1/2} \|\mathbf{v}_0\|_{1,\Omega} \leq (\mu^E)^{-1/2} \|p_0\|_{0,\Omega}$. Thus, we have

$$\begin{aligned} B_E((\mathbf{u}, \boldsymbol{\omega}, p), (\mathbf{v}_0, \mathbf{0}, 0)) &\geq \frac{C_\Omega}{\mu^E} \|p_0\|_{0,\Omega}^2 - \sqrt{\mu} (\boldsymbol{\omega}, \mathbf{curl} \mathbf{v}_0)_{0,\Omega} \\ &\geq \left(C_\Omega - \frac{1}{2\epsilon} \right) \frac{1}{\mu^E} \|p_0\|_{0,\Omega}^2 - \frac{\epsilon}{2} \|\boldsymbol{\omega}\|_{0,\Omega}^2. \end{aligned}$$

Choosing $\mathbf{v} = -\mathbf{u}$, $\boldsymbol{\theta} = \boldsymbol{\omega}$, and $q = p$, we arrive at

$$B_E((\mathbf{u}, \boldsymbol{\omega}, p), (-\mathbf{u}, \boldsymbol{\omega}, p)) = \|\boldsymbol{\omega}\|_{0,\Omega}^2 + (2\mu^E + \lambda^E)^{-1} \|p\|_{0,\Omega}^2.$$

Next, we can select $\mathbf{v} = \mathbf{0}$, $\boldsymbol{\theta} = -\sqrt{\mu^E} \mathbf{curl} \mathbf{u}$, and $q = \mu^E \operatorname{div} \mathbf{u}$, which leads to

$$\begin{aligned} B_E((\mathbf{u}, \boldsymbol{\omega}, p), (\mathbf{0}, -\sqrt{\mu^E} \mathbf{curl} \mathbf{u}, \mu^E \operatorname{div} \mathbf{u})) &\geq \frac{\mu^E}{2} \|\mathbf{curl} \mathbf{u}\|_{0,\Omega}^2 \\ &+ \frac{\mu^E}{2} \|\operatorname{div} \mathbf{u}\|_{0,\Omega}^2 - \frac{1}{2} \|\boldsymbol{\omega}\|_{0,\Omega}^2 - \frac{\mu^E}{2(2\mu^E + \lambda^E)^2} \|p\|_{0,\Omega}^2. \end{aligned}$$

We can also take $\mathbf{v} = -\mathbf{u} + \delta_1 \mathbf{v}_0$, $\boldsymbol{\theta} = \boldsymbol{\omega} - \delta_2 \sqrt{\mu^E} \mathbf{curl} \mathbf{u}$, together with $q = p + \delta_2 \mu^E \operatorname{div} \mathbf{u}$, giving

$$\begin{aligned} B_E((\mathbf{u}, \boldsymbol{\omega}, p), (\mathbf{v}, \boldsymbol{\theta}, q)) &= B_E((\mathbf{u}, \boldsymbol{\omega}, p), (-\mathbf{u}, \mathbf{0}, 0)) + \delta_1 B_E((\mathbf{u}, \boldsymbol{\omega}, p), (\mathbf{v}_0, \mathbf{0}, 0)) \\ &\quad - \delta_2 B_E((\mathbf{u}, \boldsymbol{\omega}, p), (\mathbf{0}, \sqrt{\mu^E} \mathbf{curl} \mathbf{u}, \mu^E \operatorname{div} \mathbf{u})) \\ &\geq \left(1 - \frac{\delta_1 \epsilon}{2} - \frac{\delta_2}{2} \right) \|\boldsymbol{\omega}\|_{0,\Omega}^2 + \delta_2 \frac{\mu^E}{2} \|\mathbf{curl} \mathbf{u}\|_{0,\Omega}^2 + \delta_2 \frac{\mu^E}{2} \|\operatorname{div} \mathbf{u}\|_{0,\Omega}^2 \\ &\quad + \delta_1 \left(C_\Omega - \frac{1}{2\epsilon} \right) \frac{1}{\mu^E} \|p_0\|_{0,\Omega}^2 + \frac{1}{2\mu^E + \lambda^E} \left(1 - \frac{\delta_2 \mu^E}{2\mu^E + \lambda^E} \right) \|p\|_{0,\Omega}^2. \end{aligned}$$

Choosing $\epsilon = 1/C_\Omega$, $\delta_1 = 1/2\epsilon$, and $\delta_2 = 1/2$, we have

$$B_E((\mathbf{u}, \boldsymbol{\omega}, p), (\mathbf{v}, \boldsymbol{\theta}, q)) \geq \min \left\{ \frac{C_\Omega^2}{2}, \frac{1}{4} \right\} \|(\mathbf{u}, \boldsymbol{\omega}, p)\|^2,$$

and the assertion of the theorem can be established by obtaining

$$\|(\mathbf{v}, \boldsymbol{\theta}, q)\|^2 = \left\| \left(-\mathbf{u} + \delta_1 \mathbf{v}_0, \boldsymbol{\omega} - \delta_2 \sqrt{\mu^E} \mathbf{curl} \mathbf{u}, p + \delta_2 \mu^E \operatorname{div} \mathbf{u} \right) \right\|^2 \leq 2 \|(\mathbf{u}, \boldsymbol{\omega}, p)\|^2 \square$$

2.2. Discrete spaces and Galerkin formulation. Let $\{\mathcal{T}_h\}_{h>0}$ be a shape-regular family of partitions of the closed domain $\bar{\Omega}$, conformed by tetrahedra (or triangles in two dimensions (2D)) K of diameter h_K , with mesh size $h := \max\{h_K : K \in \mathcal{T}_h\}$. We specify for any $k \geq 0$ the finite-dimensional subspaces of the functional spaces for displacement, pressure, and rotation; as follows:

$$\mathbf{V}_h := \{\mathbf{v}_h \in \mathbf{C}(\bar{\Omega}) \cap \mathbf{H}_0^1(\Omega) : \mathbf{v}_h|_K \in \mathbb{P}_{k+1}(K)^d \ \forall K \in \mathcal{T}_h\},$$

$$\begin{aligned}\mathbf{W}_h &:= \{\boldsymbol{\theta}_h \in \mathbf{L}^2(\Omega) : \boldsymbol{\theta}_h|_T \in \mathbb{P}_k(K)^{d(d-1)/2} \forall K \in \mathcal{T}_h\}, \\ Z_h &:= \{q_h \in \mathbf{L}^2(\Omega) : q_h|_T \in \mathbb{P}_k(K) \forall K \in \mathcal{T}_h\}.\end{aligned}$$

The discrete weak formulation reads as follows: find $(\mathbf{u}_h, \boldsymbol{\omega}_h, p_h) \in \mathbf{V}_h \times \mathbf{W}_h \times Z_h$ such that

$$(2.3) \quad B_E((\mathbf{u}_h, \boldsymbol{\omega}_h, p_h), (\mathbf{v}, \boldsymbol{\theta}, q)) = -(\mathbf{f}^E, \mathbf{v})_{0,\Omega} \quad \forall (\mathbf{v}, \boldsymbol{\theta}, q) \in \mathbf{V}_h \times \mathbf{W}_h \times Z_h.$$

In view of the comment above regarding pressure uniqueness in the nearly incompressible limit, we can either add a real Lagrange multiplier to fix the mean value of pressure, or (for the specific case of discontinuous pressures) simply add a jump stabilization (from, e.g., [28]). Then, for $k \geq 0$, the modified discrete weak formulation of the rotation based elasticity reads as follows: find $(\mathbf{u}_h, \boldsymbol{\omega}_h, q_h) \in \mathbf{V}_h \times \mathbf{W}_h \times Z_h$ such that

$$(2.4) \quad \begin{aligned}B_E((\mathbf{u}_h, \boldsymbol{\omega}_h, p_h), (\mathbf{v}, \boldsymbol{\theta}, q)) + \mu^{-1} \sum_{e \in \mathcal{E}(\mathcal{T}_h)} h_e \int_e [\![p_h]\!] [\!q]\!] = -(\mathbf{f}^E, \mathbf{v})_{0,\Omega} \\ \forall (\mathbf{v}, \boldsymbol{\theta}, q) \in \mathbf{V}_h \times \mathbf{W}_h \times Z_h,\end{aligned}$$

where h_e stands for the diameter of a given edge, $[\![\cdot]\!]$ the edge jump, $\mu > 0$ is a stabilization parameter, and $\mathcal{E}(\mathcal{T}_h)$ denotes the set of all edges in \mathcal{T}_h .

By repeating the arguments in Theorem 2.1, we have that (2.3) and (2.4) are well-posed. In addition, by using standard arguments, it is possible to establish the corresponding Céa's estimate and the a priori estimates.

2.3. A posteriori error analysis. First, we define the local elastic error estimator Θ_K and the elastic data oscillation $\tilde{\Upsilon}_K$ for each $K \in \mathcal{T}_h$ as

$$\begin{aligned}\Theta_K^2 &:= \frac{h_K^2}{\mu^E} \|\mathbf{R}_1\|_{0,K}^2 + \sum_{e \in \partial K} \frac{h_e}{\mu^E} \|\mathbf{R}_e\|_{0,e}^2 + \|\mathbf{R}_2\|_{0,K}^2 + \frac{1}{\frac{1}{\mu^E} + \frac{1}{2\mu^E + \lambda^E}} \|R_3\|_{0,K}^2, \\ \tilde{\Upsilon}_K^2 &:= \frac{h_K^2}{\mu^E} \|\mathbf{f}^E - \mathbf{f}_h^E\|_{0,K}^2,\end{aligned}$$

where $\mathbf{f}_h^E \in \mathbf{L}^2(\Omega)$ is a piecewise polynomial approximation of \mathbf{f}^E . Moreover, the elementwise residuals are

$$\begin{aligned}\mathbf{R}_1 &:= \{\mathbf{f}_h^E - \sqrt{\mu^E} \mathbf{curl} \boldsymbol{\omega}_h - \nabla p_h\}_K, \quad \mathbf{R}_2 := \{\boldsymbol{\omega}_h - \sqrt{\mu^E} \mathbf{curl} \mathbf{u}_h\}_K, \\ R_3 &:= \{\operatorname{div} \mathbf{u}_h + (2\mu^E + \lambda^E)^{-1} p_h\}_K,\end{aligned}$$

and the edge residual is defined as

$$\mathbf{R}_e := \begin{cases} \frac{1}{2} [\![\sqrt{\mu^E} \boldsymbol{\omega}_h \times \mathbf{n} + p_h \mathbf{n}]\!]_e, & e \in \mathcal{E}(\mathcal{T}_h) \setminus \Gamma, \\ 0, & e \in \Gamma. \end{cases}$$

Finally, the global elastic residual error estimator Θ and the global elastic data oscillation term are defined as

$$(2.5) \quad \Theta^2 := \sum_{K \in \mathcal{T}_h} \Theta_K^2, \quad \tilde{\Upsilon}^2 := \sum_{K \in \mathcal{T}_h} \tilde{\Upsilon}_K^2.$$

2.3.1. Reliability estimate. Using the Clément interpolation estimate, the following results hold:

$$(2.6) \quad h_K^{-1} \sqrt{\mu^E} \|v - I_h(v)\|_{0,K} \lesssim \sqrt{\mu^E} |v|_{1,\omega_K}, \quad h_e^{-1/2} \sqrt{\mu^E} \|v - I_h(v)\|_{0,e} \lesssim \sqrt{\mu^E} |v|_{1,\omega_K}.$$

In the next theorem, we discuss the reliability bound of the estimator Θ . The Clément interpolation estimate and the stability estimate are the main ingredients in the proof.

THEOREM 2.2 (reliability estimate for the elasticity problem). *Let $(\mathbf{u}, \boldsymbol{\omega}, p)$ be the solution to (2.2), and let $(\mathbf{u}_h, \boldsymbol{\omega}_h, p_h)$ be the solution to (2.3) (or (2.4)). Let $\Theta, \tilde{\Upsilon}$ be as in (2.5). Then*

$$(2.7) \quad \|(\mathbf{u} - \mathbf{u}_h, \boldsymbol{\omega} - \boldsymbol{\omega}_h, p - p_h)\| \leq C_{\text{rel}}(\Theta + \tilde{\Upsilon}).$$

Proof. Since $(\mathbf{u} - \mathbf{u}_h, \boldsymbol{\omega} - \boldsymbol{\omega}_h, p - p_h) \in \mathbf{H}_0^1(\Omega) \times \mathbf{L}^2(\Omega) \times \mathbf{L}^2(\Omega)$, the stability theorem, Theorem 2.1, implies

$$C_1 \|(\mathbf{u} - \mathbf{u}_h, \boldsymbol{\omega} - \boldsymbol{\omega}_h, p - p_h)\|^2 \leq B_E((\mathbf{u} - \mathbf{u}_h, \boldsymbol{\omega} - \boldsymbol{\omega}_h, p - p_h), (\mathbf{v}, \boldsymbol{\theta}, q)),$$

with $\|(\mathbf{v}, \boldsymbol{\theta}, q)\| \leq C_2 \|(\mathbf{u} - \mathbf{u}_h, \boldsymbol{\omega} - \boldsymbol{\omega}_h, p - p_h)\|$. Using the definition of the weak forms, it follows that

$$\begin{aligned} B_E((\mathbf{u} - \mathbf{u}_h, \boldsymbol{\omega} - \boldsymbol{\omega}_h, p - p_h), (\mathbf{v}, \boldsymbol{\theta}, q)) &= B_E((\mathbf{u} - \mathbf{u}_h, \boldsymbol{\omega} - \boldsymbol{\omega}_h, p - p_h), (\mathbf{v} - \mathbf{v}_h, \boldsymbol{\theta}, q)) \\ &= -(\mathbf{f}^E - \mathbf{f}_h^E, \mathbf{v} - \mathbf{v}_h)_{0,\Omega} - (\mathbf{f}_h^E, \mathbf{v} - \mathbf{v}_h)_{0,\Omega} - B_E((\mathbf{u}_h, \boldsymbol{\omega}_h, p_h), (\mathbf{v} - \mathbf{v}_h, \boldsymbol{\theta}, q)). \end{aligned}$$

Integration by parts, the Cauchy–Schwarz inequality, and the approximation results (cf. (2.6)), imply the bound

$$B_E((\mathbf{u} - \mathbf{u}_h, \boldsymbol{\omega} - \boldsymbol{\omega}_h, p - p_h), (\mathbf{v}, \boldsymbol{\theta}, q)) \leq C(\Theta + \tilde{\Upsilon}) \|(\mathbf{v}, \boldsymbol{\theta}, q)\|,$$

which, in turn, implies (2.7). \square

2.3.2. Efficiency bounds. Let $K \in \mathcal{T}_h$ and consider the interior polynomial bubble function b_K (positive in the interior of K and vanishing on ∂K). From [39], the following estimates hold:

$$(2.8) \quad \|v\|_{0,K} \lesssim \|b_K^{1/2} v\|_{0,K}, \quad \|b_K v\|_{0,K} \lesssim \|v\|_{0,K}, \quad \|\nabla(b_K v)\|_{0,K} \lesssim h_K^{-1} \|v\|_{0,K},$$

where v is a scalar-valued polynomial function defined on K .

Each term defining Θ_K in terms of local errors is bounded using the following collection of results.

LEMMA 2.1. *The following holds:*

$$h_K^2 (\mu^E)^{-1} \|\mathbf{R}_1\|_{0,K}^2 \lesssim (\mu^E)^{-1/2} h_K \|\mathbf{f}^E - \mathbf{f}_h^E\|_{0,K} + (\mu^E)^{-1/2} \|p - p_h\|_{0,K} + \|\boldsymbol{\omega} - \boldsymbol{\omega}_h\|_{0,K}.$$

Proof. For each $K \in \mathcal{T}_h$, we can define $\zeta|_K = (\mu^E)^{-1} h_K^2 \mathbf{R}_1 b_K$. We can then employ (2.8) to arrive at

$$h_K^2 (\mu^E)^{-1} \|\mathbf{R}_1\|_{0,K}^2 \lesssim \int_K \mathbf{R}_1 \cdot ((\mu^E)^{-1} h_K^2 \mathbf{R}_1 b_K) = \int_K \mathbf{R}_1 \cdot \zeta.$$

Recall that $\mathbf{f}^E - \sqrt{\mu^E} \operatorname{curl} \boldsymbol{\omega} - \nabla p = \mathbf{0}$. We subtract this from the last term and then integrate using $\zeta|_{\partial K} = \mathbf{0}$,

$$h_K^2 (\mu^E)^{-1} \|\mathbf{R}_1\|_{0,K}^2 \lesssim \int_K (\mathbf{f}_h^E - \mathbf{f}^E) \cdot \zeta + \sqrt{\mu^E} \int_K (\boldsymbol{\omega} - \boldsymbol{\omega}_h) \cdot \operatorname{curl} \zeta + \int_K (p - p_h) \nabla \cdot \zeta.$$

Then, the Cauchy–Schwarz inequality gives

$$\begin{aligned} h_K^2(\mu^E)^{-1}\|\mathbf{R}_h\|_{0,K}^2 &\lesssim (\mu^E)^{-1/2}h_K\|\mathbf{f}^E - \mathbf{f}_h^E\|_{0,K} + (\mu^E)^{-1/2}\|p - p_h\|_{0,K} \\ &+ \|\boldsymbol{\omega} - \boldsymbol{\omega}_h\|_{0,K}((\mu^E)^{1/2}\|\nabla\boldsymbol{\zeta}\|_{0,K} + (\mu^E)^{1/2}h_K^{-1}\|\boldsymbol{\zeta}\|_{0,K}). \end{aligned}$$

And the proof can be completed thanks to the following estimate:

$$\begin{aligned} (\mu^E)^{1/2}\|\nabla\boldsymbol{\zeta}\|_{0,K} + (\mu^E)^{1/2}h_K^{-1}\|\boldsymbol{\zeta}\|_{0,K} &\lesssim (\mu^E)^{1/2}(\|\nabla\boldsymbol{\zeta}\|_{0,K} + h_K^{-1}\|\boldsymbol{\zeta}\|_{0,K}) \\ &\lesssim (\mu^E)^{1/2}h_K^{-1}\|\boldsymbol{\zeta}\|_{0,K} = h_K(\mu^E)^{-1/2}\|\mathbf{R}_1\|_{0,K}. \end{aligned} \quad \square$$

LEMMA 2.2. *The following holds:*

$$\|\mathbf{R}_2\|_{0,K} \lesssim \|\boldsymbol{\omega} - \boldsymbol{\omega}_h\|_{0,K} + \sqrt{\mu^E}\|\mathbf{curl}(\mathbf{u} - \mathbf{u}_h)\|_{0,K}.$$

Proof. The constitutive relation $\boldsymbol{\omega} - \sqrt{\mu^E}\mathbf{curl}\mathbf{u} = \mathbf{0}$ implies that

$$\begin{aligned} \|\mathbf{R}_2\|_{0,K} &= \|\boldsymbol{\omega}_h - \sqrt{\mu^E}\mathbf{curl}\mathbf{u}_h\|_{0,K} = \|(\boldsymbol{\omega}_h - \boldsymbol{\omega}) - \sqrt{\mu^E}(\mathbf{curl}\mathbf{u}_h - \mathbf{curl}\mathbf{u})\|_{0,K} \\ &\lesssim \|\boldsymbol{\omega} - \boldsymbol{\omega}_h\|_{0,K} + \sqrt{\mu^E}\|\mathbf{curl}(\mathbf{u} - \mathbf{u}_h)\|_{0,K}. \end{aligned} \quad \square$$

LEMMA 2.3. *The following holds:*

$$\begin{aligned} ((\mu^E)^{-1} + (2\mu^E + \lambda^E)^{-1})^{-1/2}\|R_3\|_{0,K} \\ \lesssim \sqrt{\mu^E}\|\operatorname{div}(\mathbf{u} - \mathbf{u}_h)\|_{0,K} + (2\mu^E + \lambda^E)^{-1/2}\|p - p_h\|_{0,K}. \end{aligned}$$

Proof. Using the expression $\operatorname{div}\mathbf{u} + (2\mu^E + \lambda^E)^{-1}p = 0$, we have

$$\begin{aligned} ((\mu^E)^{-1} + (2\mu^E + \lambda^E)^{-1})^{-1/2}\|R_3\|_{0,K} &= ((\mu^E)^{-1} + (2\mu^E + \lambda^E)^{-1})^{-1/2}\|\operatorname{div}\mathbf{u}_h \\ &+ (2\mu^E + \lambda^E)^{-1}p_h\|_{0,K} \\ &\lesssim \sqrt{\mu^E}\|\operatorname{div}(\mathbf{u} - \mathbf{u}_h)\|_{0,K} + (2\mu^E + \lambda^E)^{-1/2}\|p - p_h\|_{0,K}. \end{aligned} \quad \square$$

Let e be an interior edge (or interior facet in three dimensions (3D)) shared by two elements K and K' . We assume that b_e , the edge polynomial bubble function on e , is positive in the interior of the patch P_e formed by $K \cup K'$, and b_e is zero on the boundary of the patch. Then, also from [39], the following estimates hold:

(2.9)

$$\|q\|_{0,e} \lesssim \|b_e^{1/2}q\|_{0,e}, \quad \|b_e q\|_{0,K} \lesssim h_e^{1/2}\|q\|_{0,e}, \quad \|\nabla(b_e q)\|_{0,K} \lesssim h_e^{-1/2}\|q\|_{0,e} \quad \forall K \in P_e,$$

where q denotes the scalar-valued polynomial function defined on the edge e .

LEMMA 2.4. *The following holds:*

$$\begin{aligned} &\left(\sum_{e \in \partial K} h_e(\mu^E)^{-1}\|\mathbf{R}_e\|_{0,e}^2 \right)^{1/2} \\ &\lesssim \sum_{K \in P_e} ((\mu^E)^{-1/2}h_K\|\mathbf{f}^E - \mathbf{f}_h^E\|_{0,K} + (\mu^E)^{-1/2}\|p - p_h\|_{0,K} + \|\boldsymbol{\omega} - \boldsymbol{\omega}_h\|_{0,K}). \end{aligned}$$

Proof. For $e \in \mathcal{E}(\mathcal{T}_h)$ we define locally $\boldsymbol{\zeta}_e = (\mu^E)^{-1}h_e\mathbf{R}_e b_e$. Therefore, relation (2.9) implies

$$h_e(\mu^E)^{-1}\|\mathbf{R}_e\|_{0,e}^2 \lesssim \int_e \mathbf{R}_e \cdot ((\mu^E)^{-1}h_e\mathbf{R}_e b_e) = \int_e \mathbf{R}_e \cdot \boldsymbol{\zeta}_e.$$

Since $\llbracket \boldsymbol{\omega} \times \mathbf{n} \rrbracket_e = \mathbf{0}$ and $\llbracket p\mathbf{n} \rrbracket_e = \mathbf{0}$, we have

$$\begin{aligned} & \int_e \llbracket \sqrt{\mu^E}(\boldsymbol{\omega}_h - \boldsymbol{\omega}) \times \mathbf{n} + (p_h - p)\mathbf{n} \rrbracket_e \cdot \boldsymbol{\zeta}_e \\ &= \sum_{K \in P_e} \int_K (\sqrt{\mu^E} \operatorname{curl}(\boldsymbol{\omega}_h - \boldsymbol{\omega}) + \nabla(p_h - p)) \cdot \boldsymbol{\zeta}_e \\ &+ \sum_{K \in P_e} \int_K (\sqrt{\mu^E}(\boldsymbol{\omega}_h - \boldsymbol{\omega}) \cdot \operatorname{curl} \boldsymbol{\zeta}_e + (p_h - p) \operatorname{div} \nabla \cdot \boldsymbol{\zeta}_e), \end{aligned}$$

where we have used integration by parts elementwise. Recalling that $\mathbf{f}^E - \sqrt{\mu^E} \operatorname{curl} \boldsymbol{\omega} - \nabla p = \mathbf{0}|_K$ gives

$$\begin{aligned} \frac{h_e}{\mu^E} \|\mathbf{R}_e\|_{0,e}^2 &\lesssim \sum_{K \in P_e} \int_K \left((\mathbf{f}_h^E - \mathbf{f}^E) \cdot \boldsymbol{\zeta}_e + \sqrt{\mu^E} \int_K (\boldsymbol{\omega}_h - \boldsymbol{\omega}) \cdot \operatorname{curl} \boldsymbol{\zeta}_e \right. \\ &\quad \left. + \int_K (p_h - p) \operatorname{div} \nabla \cdot \boldsymbol{\zeta}_e \right) + \sum_{K \in P_e} \int_K \mathbf{R}_1 \cdot \boldsymbol{\zeta}_e. \end{aligned}$$

From the Cauchy–Schwarz inequality we can then infer that

$$\begin{aligned} h_e(\mu^E)^{-1} \|\mathbf{R}_e\|_{0,e}^2 &\lesssim \sum_{K \in P_e} ((\mu^E)^{-1/2} h_K \|\mathbf{f}^E - \mathbf{f}_h^E\|_{0,K} + (\mu^E)^{-1/2} \|p - p_h\|_{0,K} \\ &\quad + \|\boldsymbol{\omega} - \boldsymbol{\omega}_h\|_{0,K}) \times ((\mu^E)^{1/2} \|\nabla \boldsymbol{\zeta}_e\|_{0,K} + (\mu^E)^{1/2} h_K^{-1} \|\boldsymbol{\zeta}_e\|_{0,K}). \end{aligned}$$

And the assertion of the lemma is proven after obtaining the bound

$$\begin{aligned} & (\mu^E)^{1/2} \|\nabla \boldsymbol{\zeta}_e\|_{0,K} + (\mu^E)^{1/2} h_K^{-1} \|\boldsymbol{\zeta}_e\|_{0,K} \\ & \lesssim (\mu^E)^{1/2} h_K^{-1} \|\boldsymbol{\zeta}_e\|_{0,K} = h_e^{1/2} (\mu^E)^{-1/2} \|\mathbf{R}_e\|_{0,e}. \quad \square \end{aligned}$$

Now, we are in position to state the efficiency of the proposed estimator Θ .

THEOREM 2.3 (efficiency estimate for the elasticity problem). *Let $(\mathbf{u}, \boldsymbol{\omega}, p)$ be the solution to (2.2) and $(\mathbf{u}_h, \boldsymbol{\omega}_h, p_h)$ the solution to (2.3) (or (2.4)). Also, let $\Theta, \tilde{\Upsilon}$ be as in (2.5). Then*

$$\Theta \leq C_{\text{eff}} (\|(\mathbf{u} - \mathbf{u}_h, \boldsymbol{\omega} - \boldsymbol{\omega}_h, p - p_h)\| + \tilde{\Upsilon}).$$

Proof. It suffices to combine Lemmas 2.1–2.4. \square

3. Rotation-based poroelasticity with total pressure. In this section we propose a mixed finite element method for the approximation of linear poroelasticity equations, formulated in terms of displacement, rotation vector, fluid pressure, and total pressure. Then, we will present an a posteriori error analysis.

3.1. Continuous formulation. We consider the steady poroelasticity equations written in terms of displacement \mathbf{u} , fluid pressure p , rescaled total pressure $\phi := \alpha p - (2\mu^P + \lambda^P) \operatorname{div} \mathbf{u}$, and rescaled rotation vector $\boldsymbol{\omega} := \sqrt{\mu^P} \operatorname{curl} \mathbf{u}$, where $\alpha > 0$ is the Biot–Willis parameter, and λ^P, μ^P are the Lamé constants. Moreover, s^P is a smooth fluid source term, κ is the permeability (isotropic and satisfying $0 < \kappa_1 \leq \kappa(\mathbf{x}) \leq \kappa_2 < \infty$ for all $\mathbf{x} \in \Omega$), $c_0 > 0$ is the storativity coefficient, \mathbf{g} is

gravity, \mathbf{f}^P is the external load, and ξ, ρ are the viscosity and density of the pore fluid, respectively. The system reads

$$(3.1a) \quad \sqrt{\mu^P} \operatorname{curl} \boldsymbol{\omega} + \nabla \phi = \mathbf{f}^P \quad \text{in } \Omega,$$

$$(3.1b) \quad \boldsymbol{\omega} - \sqrt{\mu^P} \operatorname{curl} \mathbf{u} = \mathbf{0} \quad \text{in } \Omega,$$

$$(3.1c) \quad (2\mu^P + \lambda^P)^{-1} \phi + \operatorname{div} \mathbf{u} - \alpha(2\mu^P + \lambda^P)^{-1} p = 0 \quad \text{in } \Omega,$$

$$(3.1d)$$

$$[c_0 + \alpha^2(\mu^P + \lambda^P)^{-1}] p - \alpha(2\mu^P + \lambda^P)^{-1} \phi - \xi^{-1} \operatorname{div} [\kappa(\nabla p - \rho \mathbf{g})] = s^P \quad \text{in } \Omega,$$

and we assume that the domain is clamped and consider zero filtration flux on the boundary

$$\mathbf{u} = \mathbf{0} \quad \text{on } \partial\Omega, \quad \kappa \xi^{-1} (\nabla p - \rho \mathbf{g}) \cdot \mathbf{n} = 0 \quad \text{on } \partial\Omega.$$

Testing each equation of (3.1a)–(3.1d), integrating by parts whenever adequate (see [25, Theorem 2.11]), and applying the boundary conditions we obtain

$$(3.2) \quad \begin{aligned} & -\sqrt{\mu^P} \int_{\Omega} \operatorname{curl} \mathbf{v} \cdot \boldsymbol{\omega} + \int_{\Omega} \phi \operatorname{div} \mathbf{v} = -\int_{\Omega} \mathbf{f}^P \cdot \mathbf{v}, \\ & \int_{\Omega} \boldsymbol{\omega} \cdot \boldsymbol{\theta} - \sqrt{\mu^P} \int_{\Omega} \boldsymbol{\theta} \cdot \operatorname{curl} \mathbf{u} = 0, \\ & (2\mu^P + \lambda^P)^{-1} \int_{\Omega} \phi \psi + \int_{\Omega} \psi \operatorname{div} \mathbf{u} - \alpha(2\mu^P + \lambda^P)^{-1} \int_{\Omega} p \psi = 0, \\ & -\left[c_0 + \frac{\alpha^2}{(2\mu^P + \lambda^P)} \right] \int_{\Omega} p q + \frac{\alpha}{2\mu^P + \lambda^P} \int_{\Omega} \phi q \\ & \quad - \int_{\Omega} \frac{\kappa}{\xi} \nabla p \cdot \nabla q = -\frac{\rho}{\xi} \int_{\Omega} \kappa \mathbf{g} \cdot \nabla q - \int_{\Omega} s^P q \end{aligned}$$

for each $(\mathbf{v}, \boldsymbol{\theta}, \psi, q) \in \mathbf{H}_0^1(\Omega) \times \mathbf{L}^2(\Omega) \times \mathbf{L}^2(\Omega) \times \mathbf{H}^1(\Omega)$.

We can regard the rotation and the rescaled total pressure ϕ as a single unknown $\vec{\omega} := (\boldsymbol{\omega}, \phi)$. This gives the unsymmetric variational form: find $(\vec{\omega}, \mathbf{u}, p) \in \mathbf{H} \times \mathbf{V} \times \mathbf{Q}$ such that

$$(3.3a) \quad a(\vec{\omega}, \vec{\theta}) + b_1(\vec{\theta}, \mathbf{u}) - b_2(\vec{\theta}, p) = 0 \quad \forall \vec{\theta} \in \mathbf{H},$$

$$(3.3b) \quad b_1(\vec{\omega}, \mathbf{v}) = F(\mathbf{v}) \quad \forall \mathbf{v} \in \mathbf{V},$$

$$(3.3c) \quad b_2(\vec{\omega}, q) - c(p, q) = G(q) \quad \forall q \in \mathbf{Q},$$

where $\vec{\theta} := (\boldsymbol{\theta}, \psi)$, $\mathbf{H} := \mathbf{L}^2(\Omega) \times \mathbf{L}^2(\Omega)$, $\mathbf{V} := \mathbf{H}_0^1(\Omega)$, $\mathbf{Q} := \mathbf{H}^1(\Omega)$, and the bilinear forms $a : \mathbf{H} \times \mathbf{H} \rightarrow \mathbb{R}$, $b_1 : \mathbf{H} \times \mathbf{V} \rightarrow \mathbb{R}$, $b_2 : \mathbf{H} \times \mathbf{Q} \rightarrow \mathbb{R}$, $b_3 : \mathbf{H} \times \mathbf{Q} \rightarrow \mathbb{R}$, $c : \mathbf{Q} \times \mathbf{Q} \rightarrow \mathbb{R}$, and linear functionals $F : \mathbf{V} \rightarrow \mathbb{R}$, $G : \mathbf{Q} \rightarrow \mathbb{R}$ are specified in the following way:

$$a(\vec{\omega}, \vec{\theta}) := \int_{\Omega} \boldsymbol{\omega} \cdot \boldsymbol{\theta} + \frac{1}{2\mu^P + \lambda^P} \int_{\Omega} \phi \psi,$$

$$b_1(\vec{\theta}, \mathbf{v}) := -\sqrt{\mu^P} \int_{\Omega} \boldsymbol{\theta} \cdot \operatorname{curl} \mathbf{v} + \int_{\Omega} \psi \operatorname{div} \mathbf{v}, \quad b_2(\vec{\theta}, p) := \frac{\alpha}{2\mu^P + \lambda^P} \int_{\Omega} p \psi,$$

$$c(p, q) := \left[c_0 + \frac{\alpha^2}{2\mu^P + \lambda^P} \right] \int_{\Omega} p q + \frac{1}{\xi} \int_{\Omega} \kappa \nabla p \cdot \nabla q, \quad F(\mathbf{v}) := -\int_{\Omega} \mathbf{f}^P \cdot \mathbf{v},$$

$$G(q) := -\frac{\rho}{\xi} \int_{\Omega} \kappa \mathbf{g} \cdot \nabla q - \int_{\Omega} s^P q.$$

Note that the displacement space $H_0(\mathbf{curl}, \Omega) \cap H_0(\operatorname{div}, \Omega)$ is algebraically and topologically equivalent to \mathbf{V} if Ω is a polyhedral bounded domain with Lipschitz boundary [25, Lemma 2.5, Remark 2.7].

The formulation in (3.3) can be also written, more concisely, as

$$B_P((\mathbf{u}, \boldsymbol{\omega}, \phi, p), (\mathbf{v}, \boldsymbol{\theta}, \psi, q)) = F(\mathbf{v}) + G(q),$$

where the multilinear form (now having a subscript P for *poroelasticity*) is defined as

$$B_P((\mathbf{u}, \boldsymbol{\omega}, \phi, p), (\mathbf{v}, \boldsymbol{\theta}, \psi, q)) := a(\vec{\boldsymbol{\omega}}, \vec{\boldsymbol{\theta}}) + b_1(\vec{\boldsymbol{\theta}}, \mathbf{u}) - b_2(\vec{\boldsymbol{\theta}}, p) + b_1(\vec{\boldsymbol{\omega}}, \mathbf{v}) + b_2(\vec{\boldsymbol{\omega}}, q) - c(p, q).$$

The following result will be useful in the next section.

THEOREM 3.1. *Assume $\frac{\alpha^2}{2\mu^P + \lambda^P} \in (0, 9c_0/10]$. For every $(\mathbf{u}, \boldsymbol{\omega}, \phi, p) \in \mathbf{H}_0^1(\Omega) \times \mathbf{L}^2(\Omega) \times \mathbf{L}^2(\Omega) \times \mathbf{H}^1(\Omega)$, there exists $(\mathbf{v}, \boldsymbol{\theta}, \psi, q) \in \mathbf{H}_0^1(\Omega) \times \mathbf{L}^2(\Omega) \times \mathbf{L}^2(\Omega) \times \mathbf{H}^1(\Omega)$ with $\|(\mathbf{v}, \boldsymbol{\theta}, \psi, q)\| \leq C_1 \|(\mathbf{u}, \boldsymbol{\omega}, \phi, p)\|$ such that*

$$B_P((\mathbf{u}, \boldsymbol{\omega}, \phi, p), (\mathbf{v}, \boldsymbol{\theta}, \psi, q)) \geq C_2 \|(\mathbf{u}, \boldsymbol{\omega}, \phi, p)\|^2,$$

where

$$\begin{aligned} \|(\mathbf{v}, \boldsymbol{\theta}, \psi, q)\|^2 &:= \mu^P (\|\mathbf{curl} \mathbf{v}\|_{0,\Omega}^2 + \|\operatorname{div} \mathbf{v}\|_{0,\Omega}^2) + \|\boldsymbol{\theta}\|_{0,\Omega}^2 + \frac{1}{\mu^P} \|\psi_0\|_{0,\Omega}^2 + \frac{1}{2\mu^P + \lambda^P} \|\psi\|_{0,\Omega}^2 \\ &\quad + \left(c_0 + \frac{\alpha^2}{2\mu^P + \lambda^P} \right) \|q\|_{0,\Omega}^2 + \left\| \frac{\kappa}{\xi} \nabla q \right\|_{0,\Omega}^2. \end{aligned}$$

Proof. Analogously as in the proof of Theorem 2.1, we have that there exists $\mathbf{v}_0 \in \mathbf{H}_0^1(\Omega)$ such that

$$\begin{aligned} B_P((\mathbf{u}, \boldsymbol{\omega}, \phi, p), (\mathbf{v}_0, \mathbf{0}, 0, 0)) &\geq \frac{C_\Omega}{\mu^P} \|\phi_0\|_{0,\Omega}^2 - \sqrt{\mu^P} (\boldsymbol{\omega}, \mathbf{curl} \mathbf{v}_0) \\ &\geq \left(C_\Omega - \frac{1}{2\epsilon} \right) \frac{1}{\mu^P} \|\phi_0\|_{0,\Omega}^2 - \frac{\epsilon}{2} \|\boldsymbol{\omega}\|_{0,\Omega}^2. \end{aligned}$$

First, we take $\mathbf{v} = -\mathbf{u}$, $\boldsymbol{\theta} = \boldsymbol{\omega}$, $\psi = \phi$, and $q = -p$. Consequently,

$$\begin{aligned} B_P((\mathbf{u}, \boldsymbol{\omega}, \phi, p), (-\mathbf{u}, \boldsymbol{\omega}, \phi, -p)) &= \|\boldsymbol{\omega}\|_{0,\Omega}^2 + (2\mu^P + \lambda^P)^{-1} \|\phi\|_{0,\Omega}^2 - 2\alpha(2\mu^P + \lambda^P)^{-1} (p, \phi)_{0,\Omega} \\ &\quad + (c_0 + \alpha^2(2\mu^P + \lambda^P)^{-1}) \|p\|_{0,\Omega}^2 + \|\kappa/\xi \nabla p\|_{0,\Omega}^2. \end{aligned}$$

Next, we choose $\mathbf{v} = \mathbf{0}$, $\boldsymbol{\theta} = -\sqrt{\mu^P} \mathbf{curl} \mathbf{u}$, $\psi = \mu^P \operatorname{div} \mathbf{u}$ and $q = 0$, and therefore,

$$\begin{aligned} B_P((\mathbf{u}, \boldsymbol{\omega}, \phi, p), (\mathbf{0}, -\sqrt{\mu^P} \mathbf{curl} \mathbf{u}, \mu^P \operatorname{div} \mathbf{u}, 0)) &= \mu^P \|\mathbf{curl} \mathbf{u}\|_{0,\Omega}^2 + \mu^P \|\operatorname{div} \mathbf{u}\|_{0,\Omega}^2 - \sqrt{\mu^P} (\boldsymbol{\omega}, \mathbf{curl} \mathbf{u}) + \mu^P (2\mu^P + \lambda^P)^{-1} (\phi, \operatorname{div} \mathbf{u}) \\ &\quad - \alpha \mu^P (2\mu^P + \lambda^P)^{-1} (p, \operatorname{div} \mathbf{u}) \\ &\geq \frac{\mu^P}{2} \|\mathbf{curl} \mathbf{u}\|_{0,\Omega}^2 + \left(1 - \frac{\mu^P}{(2\mu^P + \lambda^P)} \right) \mu^P \|\operatorname{div} \mathbf{u}\|_{0,\Omega}^2 - \frac{1}{2} \|\boldsymbol{\omega}\|_{0,\Omega}^2 \end{aligned}$$

$$-\frac{\alpha^2}{2(2\mu^P + \lambda^P)} \|p\|_{0,\Omega}^2 - \frac{1}{2(2\mu^P + \lambda^P)} \|\phi\|_{0,\Omega}^2.$$

Finally, we can take $\mathbf{v} = -\mathbf{u} + \delta_1 \mathbf{v}_0$, $\boldsymbol{\theta} = \boldsymbol{\omega} - \delta_2 \sqrt{\mu^P} \operatorname{curl} \mathbf{u}$, $\psi = \phi + \delta_2 \mu^P \operatorname{div} \mathbf{u}$, and $q = -p$ to obtain

$$\begin{aligned} B_P((\mathbf{u}, \boldsymbol{\omega}, \phi, p), (\mathbf{v}, \boldsymbol{\theta}, \psi, q)) &= B_P((\mathbf{u}, \boldsymbol{\omega}, \phi, p), (-\mathbf{u}, \boldsymbol{\omega}, \phi, -p)) \\ &\quad + \delta_1 B_P((\mathbf{u}, \boldsymbol{\omega}, \phi, p), (\mathbf{v}_0, \mathbf{0}, 0, 0)) \\ &\quad + \delta_2 B_P((\mathbf{u}, \boldsymbol{\omega}, \phi, p), (\mathbf{0}, -\sqrt{\mu^P} \operatorname{curl} \mathbf{u}, \mu^P \operatorname{div} \mathbf{u}, 0)) \\ &\geq \left(1 - \frac{\delta_1 \epsilon}{2} - \frac{\delta_2}{2}\right) \|\boldsymbol{\omega}\|_{0,\Omega}^2 + \frac{\mu^P \delta_2}{2} \|\operatorname{curl} \mathbf{u}\|_{0,\Omega}^2 + \delta_1 \left(1 - \frac{\mu^P}{(2\mu^P + \lambda^P)}\right) \|\operatorname{div} \mathbf{u}\|_{0,\Omega}^2 \\ &\quad + \left(C_\Omega - \frac{1}{2\epsilon}\right) \frac{\delta_1}{\mu^P} \|\phi_0\|_{0,\Omega}^2 + \frac{1}{2\mu^P + \lambda^P} \left(\frac{1}{2} - \frac{\delta_2}{2}\right) \|\phi\|_{0,\Omega}^2 + \|\kappa/\xi \nabla p\|_{0,\Omega}^2 \\ &\quad + \left(c_0 + \frac{\alpha^2}{(2\mu^P + \lambda^P)} \left(-1 - \frac{\delta_2}{2}\right)\right) \|p\|_{0,\Omega}^2. \end{aligned}$$

Choosing $\epsilon = 1/C_\Omega$, $\delta_1 = 1/2\epsilon$, and $\delta_2 = 1/5$, we have

$$B_P((\mathbf{u}, \boldsymbol{\omega}, \phi, p), (\mathbf{v}, \boldsymbol{\theta}, \psi, q)) \geq \frac{1}{4} \min \left\{ C_\Omega^2, \frac{1}{50} \right\} \|(\mathbf{u}, \boldsymbol{\omega}, \phi, p)\|^2.$$

And from that, the following estimate completes the proof:

$$\begin{aligned} \|(\mathbf{v}, \boldsymbol{\theta}, \psi, q)\|^2 &= \|(-\mathbf{u} + \delta_1 \mathbf{v}_0, \boldsymbol{\omega} - \delta_2 \sqrt{\mu^P} \operatorname{curl} \mathbf{u}, \phi + \delta_2 \mu^P \operatorname{div} \mathbf{u}, -p)\|^2 \\ &\leq 2 \|(\mathbf{u}, \boldsymbol{\omega}, \phi, p)\|^2. \end{aligned}$$

□

3.2. Discrete spaces and Galerkin formulation. With the same notation as in section 2.2, we specify finite-dimensional subspaces of the functional spaces for displacement, fluid pressure, rotations, and total pressure as follows:

$$\begin{aligned} \mathbf{V}_h &:= \{\mathbf{v}_h \in \mathbf{C}(\bar{\Omega}) \cap \mathbf{V} : \mathbf{v}_h|_K \in \mathbb{P}_{k+1}(K)^d \ \forall K \in \mathcal{T}_h\}, \\ Q_h &:= \{q_h \in \mathbf{C}(\bar{\Omega}) \cap \mathbf{Q} : q_h|_K \in \mathbb{P}_{k+1}(K) \ \forall K \in \mathcal{T}_h\}, \\ \mathbf{W}_h &:= \{\boldsymbol{\theta}_h \in \mathbf{L}^2(\Omega) : \boldsymbol{\theta}_h|_K \in \mathbb{P}_k(K)^{d(d-1)/2} \ \forall K \in \mathcal{T}_h\}, \\ (3.4) \quad Z_h &:= \{\psi_h \in \mathbf{L}^2(\Omega) : \psi_h|_K \in \mathbb{P}_k(K) \ \forall K \in \mathcal{T}_h\}. \end{aligned}$$

Then the discrete formulation consists of finding $(\mathbf{u}_h, \boldsymbol{\omega}_h, \phi_h, p_h) \in \mathbf{V}_h \times \mathbf{W}_h \times Z_h \times Q_h$ such that

$$(3.5) \quad B_P((\mathbf{u}_h, \boldsymbol{\omega}_h, \phi_h, p_h), (\mathbf{v}, \boldsymbol{\theta}, \psi, q)) = F(\mathbf{v}) + G(q)$$

for all $(\mathbf{v}, \boldsymbol{\theta}, \psi, q) \in \mathbf{V}_h \times \mathbf{W}_h \times Z_h \times Q_h$. Likewise, for each $k \geq 0$, the modified (stabilized) discrete weak formulation of the rotation based poroelasticity is as follows: find $(\mathbf{u}_h, \boldsymbol{\omega}_h, \phi_h, p_h) \in \mathbf{V}_h \times \mathbf{W}_h \times Z_h \times Q_h$ such that

$$\begin{aligned} (3.6) \quad B_P((\mathbf{u}_h, \boldsymbol{\omega}_h, \phi_h, p_h), (\mathbf{v}, \boldsymbol{\theta}, \psi, q)) + \mu^{-1} \sum_{e \in \mathcal{E}(\mathcal{T}_h)} h_e \int_e [\![\phi_h]\!] [\!\psi]\!] \\ = -(\mathbf{f}^P, \mathbf{v})_{0,\Omega} - \frac{\rho}{\xi} (\kappa \mathbf{g}, \nabla q)_{0,\Omega} - (s^P, q)_{0,\Omega} \end{aligned}$$

for all $(\mathbf{v}, \boldsymbol{\theta}, \psi, q) \in \mathbf{V}_h \times \mathbf{W}_h \times Z_h \times Q_h$.

The analysis of the continuous and discrete formulations is not found in [5, 4]. For the sake of completeness, we outline it in Appendices A and B.

3.3. A posteriori error analysis. First, we define the poroelastic local error estimator Ψ_K as

$$\begin{aligned}\Psi_K^2 := & \frac{h_K^2}{\mu^P} \|\mathbf{R}_1\|_{0,K}^2 + \sum_{e \in \partial K} \frac{h_e}{\mu^P} \|\mathbf{R}_e\|_{0,e}^2 + \|\mathbf{R}_2\|_{0,K}^2 + \rho_d \|R_3\|_{0,K}^2 + \rho_1 \|R_4\|_{0,K}^2 \\ & + \sum_{e \in \partial K} \rho_2 \|R_e\|_{0,e}^2,\end{aligned}$$

where the elemental residuals are defined as

$$\begin{aligned}\mathbf{R}_1 &:= \{\mathbf{f}_h^P - \sqrt{\mu^P} \operatorname{curl} \boldsymbol{\omega}_h - \nabla \phi_h\}_K, \quad \mathbf{R}_2 := \{\boldsymbol{\omega}_h - \sqrt{\mu^P} \operatorname{curl} \mathbf{u}_h\}_K, \\ R_3 &:= \{\operatorname{div} \mathbf{u}_h + (2\mu^P + \lambda^P)^{-1} \phi_h - \alpha(2\mu + \lambda^P)^{-1} p_h\}_K, \\ R_4 &:= \{s_h^P - (c_0 + \alpha^2(2\mu + \lambda)^{-1}) p_h + \alpha(2\mu^P + \lambda^P)^{-1} \phi_h + \xi^{-1} \operatorname{div} [\kappa(\nabla p_h - \rho \mathbf{g})]\}_K,\end{aligned}$$

and the edge residuals are defined as

$$\begin{aligned}\mathbf{R}_e &:= \begin{cases} \frac{1}{2} [\sqrt{\mu^P} \boldsymbol{\omega}_h \times \mathbf{n} + \phi_h \mathbf{n}]_e, & e \in \mathcal{E}(\mathcal{T}_h) \setminus \Gamma, \\ 0, & e \in \Gamma, \end{cases} \\ R_e &:= \begin{cases} \frac{1}{2} [\xi^{-1} \kappa(\nabla p_h - \rho \mathbf{g})]_e, & e \in \mathcal{E}(\mathcal{T}_h) \setminus \Gamma, \\ \xi^{-1} \kappa(\nabla p_h - \rho \mathbf{g}), & e \in \Gamma, \end{cases}\end{aligned}$$

with the scaling constants taken as

$$\begin{aligned}\rho_1 &:= \min\{(c_0 + \alpha^2(2\mu^P + \lambda^P)^{-1})^{-1}, h_K^2 \xi \kappa^{-1}\}, \\ \rho_2 &:= \xi \kappa^{-1} h_e, \quad \rho_d := ((\mu^P)^{-1} + (2\mu^P + \lambda^P)^{-1})^{-1}.\end{aligned}$$

On the other hand, the definition of the poroelastic oscillation term $\widehat{\Upsilon}_K$ is as follows:

$$\widehat{\Upsilon}_K^2 = h_K^2 (\mu^P)^{-1} \|\mathbf{f}^P - \mathbf{f}_h^P\|_{0,K}^2 + \rho_1 \|s^P - s_h^P\|_{0,K}^2.$$

Finally, the global residual error estimator and data oscillation terms are, respectively,

$$(3.7) \quad \Psi^2 := \sum_{K \in \mathcal{T}_h} \Psi_K^2, \quad \widehat{\Upsilon}^2 := \sum_{K \in \mathcal{T}_h} \widehat{\Upsilon}_K^2.$$

3.3.1. Reliability. In this section, we establish reliability of (3.7). The main ingredients are the stability theorem and the interpolation estimate to establish the upper bound.

THEOREM 3.2 (reliability for the Biot problem). *Let $(\mathbf{u}, \boldsymbol{\omega}, \phi, p)$ and $(\mathbf{u}_h, \boldsymbol{\omega}_h, \phi_h, p_h)$ be the solutions of the weak formulations (3.2) and (3.5) (or (3.6)), respectively. Then the following reliability bound holds:*

$$\|(\mathbf{u} - \mathbf{u}_h, \boldsymbol{\omega} - \boldsymbol{\omega}_h, \phi - \phi_h, p - p_h)\| \leq C_{\text{rel}} (\Psi + \widehat{\Upsilon}),$$

where $C_{\text{rel}} > 0$ is a positive constant independent of mesh size and parameters.

Proof. Since $(\mathbf{u} - \mathbf{u}_h, \boldsymbol{\omega} - \boldsymbol{\omega}_h, \phi - \phi_h, p - p_h) \in \mathbf{H}_0^1(\Omega) \times \mathbf{L}^2(\Omega) \times \mathbf{L}^2(\Omega) \times \mathbf{H}^1(\Omega)$, Theorem 3.1 then implies

$$C_2 \|(\mathbf{u} - \mathbf{u}_h, \boldsymbol{\omega} - \boldsymbol{\omega}_h, \phi - \phi_h, p - p_h)\|^2 \leq B_P((\mathbf{u} - \mathbf{u}_h, \boldsymbol{\omega} - \boldsymbol{\omega}_h, \phi - \phi_h, p - p_h), (\mathbf{v}, \boldsymbol{\theta}, \psi, q)),$$

with $\|(\mathbf{v}, \boldsymbol{\theta}, \psi, q)\| \leq C_1 \|(\mathbf{u} - \mathbf{u}_h, \boldsymbol{\omega} - \boldsymbol{\omega}_h, \phi - \phi_h, p - p_h)\|$. From the definition of B_P , it follows that

$$\begin{aligned} & B_P((\mathbf{u} - \mathbf{u}_h, \boldsymbol{\omega} - \boldsymbol{\omega}_h, \phi - \phi_h, p - p_h), (\mathbf{v}, \boldsymbol{\theta}, \psi, q)) \\ &= -(\mathbf{f}^P - \mathbf{f}_h^P, \mathbf{v} - \mathbf{v}_h)_{0,\Omega} - \rho \xi^{-1} (\kappa \mathbf{g}, \nabla(q - q_h))_{0,\Omega} \\ &\quad + (s^P - s_h^P, q - q_h)_{0,\Omega} - (\mathbf{f}_h^P, \mathbf{v} - \mathbf{v}_h)_{0,\Omega} + (s_h^P, q - q_h)_{0,\Omega} \\ &\quad - B_P((\mathbf{u}_h, \boldsymbol{\omega}_h, \phi_h, p_h), (\mathbf{v} - \mathbf{v}_h, \boldsymbol{\theta}, \psi, q - q_h)). \end{aligned}$$

Finally, applying integration by parts, the Cauchy–Schwarz inequality, and approximation results yields

$$B_P((\mathbf{u} - \mathbf{u}_h, \boldsymbol{\omega} - \boldsymbol{\omega}_h, \phi - \phi_h, p - p_h), (\mathbf{v}, \boldsymbol{\theta}, \psi, q)) \leq C(\Psi + \widehat{\Upsilon}) \|(\mathbf{v}, \boldsymbol{\theta}, \psi, q)\|. \quad \square$$

3.3.2. Efficiency. The following lemmas provide upper bounds for each term defining Ψ_K .

LEMMA 3.1. *The following holds:*

$$h_K(\mu^P)^{-1/2} \|\mathbf{R}_1\|_{0,K}^2 \lesssim (\mu^P)^{-1/2} h_K \|\mathbf{f}^P - \mathbf{f}_h^P\|_{0,K} + (\mu^P)^{-1/2} \|\phi - \phi_h\|_{0,K} + \|\boldsymbol{\omega} - \boldsymbol{\omega}_h\|_{0,K}.$$

Proof. The proof follows from Lemma 2.1. \square

LEMMA 3.2. *The following holds:*

$$\|\mathbf{R}_2\|_{0,K} \lesssim \|\boldsymbol{\omega} - \boldsymbol{\omega}_h\|_{0,K} + \sqrt{\mu^P} \|\operatorname{curl}(\mathbf{u} - \mathbf{u}_h)\|_{0,K}.$$

Proof. The proof follows from Lemma 2.2. \square

LEMMA 3.3. *The following holds:*

$$\begin{aligned} \rho_d^{1/2} \|\mathbf{R}_3\|_{0,K} &\lesssim \sqrt{\mu^P} \|\operatorname{div}(\mathbf{u} - \mathbf{u}_h)\|_{0,K} + (2\mu^P + \lambda^P)^{-1/2} \|\phi - \phi_h\|_{0,K} \\ &\quad + \alpha(2\mu^P + \lambda^P)^{-1/2} \|p - p_h\|_{0,K}. \end{aligned}$$

Proof. Using the expression $\operatorname{div} \mathbf{u} + (2\mu^P + \lambda^P)^{-1}\phi - \alpha(2\mu^P + \lambda^P)^{-1}p = 0$, we have

$$\begin{aligned} \rho_d^{1/2} \|\mathbf{R}_3\|_{0,K} &= \rho_d^{1/2} \|\operatorname{div} \mathbf{u}_h + (2\mu^P + \lambda^P)^{-1}\phi_h - \alpha(2\mu^P + \lambda^P)^{-1}p_h\|_{0,K} \\ &\lesssim \sqrt{\mu^P} \|\operatorname{div}(\mathbf{u} - \mathbf{u}_h)\|_{0,K} + (2\mu^P + \lambda^P)^{-1/2} \|\phi - \phi_h\|_{0,K} \\ &\quad + \alpha(2\mu^P + \lambda^P)^{-1/2} \|p - p_h\|_{0,K}. \end{aligned} \quad \square$$

LEMMA 3.4. *The following holds:*

$$\begin{aligned} h_K(\mu^P)^{-1/2} \|R_4\|_{0,K}^2 &\lesssim (\rho_1)^{1/2} \|s^P - s_h^P\|_{0,K} + [c_0 + \alpha^2(2\mu + \lambda)^{-1}]^{1/2} \|p - p_h\|_{0,K} \\ &\quad + (\kappa/\xi)^{1/2} \|\nabla(p - p_h)\|_{0,K} \\ &\quad + (2\mu^P + \lambda^P)^{-1/2} \|\phi - \phi_h\|_{0,K}. \end{aligned}$$

Proof. For each $K \in \mathcal{T}_h$, we can take $\zeta|_K = (\rho_1)^{-1} R_4 b_K$. Then, invoking (2.8), we end up with

$$(\rho_1)^{-1} \|R_4\|_{0,K}^2 \lesssim \int_K R_4 ((\rho_1)^{-1} R_4 b_K) = \int_K R_4 \zeta.$$

Recall that $s - [c_0 + \alpha^2(2\mu + \lambda)^{-1}]p + \alpha(2\mu^P + \lambda^P)^{-1}\phi + \xi^{-1} \operatorname{div}[\kappa(\nabla p - \rho\mathbf{g})]_K = 0$. We subtract this from the last term, and then integrate using $\zeta|_{\partial K} = \mathbf{0}$ to obtain

$$\begin{aligned} (\rho_1)^{-1}\|R_4\|_{0,K}^2 &\lesssim \int_K (s_h^P - s^P)\zeta + [c_0 + \alpha^2(2\mu + \lambda)^{-1}] \int_K (p - p_h)\zeta \\ &\quad + \xi^{-1} \int_K \kappa \nabla(p - p_h) \cdot \nabla \zeta \\ &\quad + \alpha(2\mu + \lambda)^{-1} \int_K (\phi - \phi_h)\zeta. \end{aligned}$$

Then, the Cauchy–Schwarz inequality gives

$$\begin{aligned} (\rho_1)^{-1}\|R_4\|_{0,K}^2 &\lesssim ((\rho_1)^{1/2}\|s^P - s_h^P\|_{0,K} + [c_0 + \alpha^2(2\mu + \lambda)^{-1}]^{1/2}\|p - p_h\|_{0,K} \\ &\quad + \xi^{-1/2}\|\kappa^{1/2}\nabla(p - p_h)\|_{0,K} \\ &\quad + (2\mu^P + \lambda^P)^{-1/2}\|\phi - \phi_h\|_{0,K})((\kappa/\xi)^{1/2}\|\nabla \zeta\|_{0,K} + (\rho_1)^{-1/2}\|\zeta\|_{0,K}). \end{aligned}$$

The proof follows after noting that

$$\begin{aligned} \left(\frac{\kappa}{\xi}\right)^{1/2}\|\nabla \zeta\|_{0,K} + (\rho_1)^{-1/2}\|\zeta\|_{0,K} &\lesssim \left(\frac{\kappa}{\xi}\right)^{1/2} h_K^{-1}\|\zeta\|_{0,K} + \rho_1^{-1/2}\|\zeta\|_{0,K} \\ &\lesssim (\rho_1)^{-1/2}\|\zeta\|_{0,K} = (\rho_1)^{1/2}\|R_4\|_{0,K}. \end{aligned} \quad \square$$

LEMMA 3.5. *The following holds:*

$$\begin{aligned} \left(\sum_{e \in \partial K} h_e(\mu^P)^{-1}\|\mathbf{R}_e\|_{0,e}^2\right)^{1/2} &\lesssim \sum_{K \in P_e} ((\mu^P)^{-1/2}h_K\|\mathbf{f}^P - \mathbf{f}_h^P\|_{0,K} \\ &\quad + (\mu^P)^{-1/2}\|\phi - \phi_h\|_{0,K} + \|\boldsymbol{\omega} - \boldsymbol{\omega}_h\|_{0,K}). \end{aligned}$$

Proof. The proof readily follows from Lemma 2.4. \square

LEMMA 3.6. *The following holds:*

$$\begin{aligned} \left(\sum_{e \in \partial K} \rho_2\|R_e\|_{0,e}^2\right)^{1/2} &\lesssim \sum_{K \in P_e} ((\rho_1)^{1/2}\|s^P - s_h^P\|_{0,K} \\ &\quad + [c_0 + \alpha^2(2\mu + \lambda)^{-1}]^{1/2}\|p - p_h\|_{0,K} + (\kappa/\xi)^{1/2}\|\nabla(p - p_h)\|_{0,K} \\ &\quad + (2\mu^P + \lambda^P)^{-1/2}\|\phi - \phi_h\|_{0,K}). \end{aligned}$$

Proof. For $e \in \mathcal{E}(\mathcal{T}_h)$ we can locally choose $\zeta_e = \rho_2 R_e b_e$. Then, from (2.9), we readily have that

$$(3.8) \quad \rho_2\|R_e\|_{0,e}^2 \lesssim \int_e R_e \cdot (\rho_2 R_e b_e) = \int_e R_e \cdot \zeta_e.$$

The weak form (3.2) leads to

$$\begin{aligned} \int_{\Omega} (\kappa/\xi) \nabla(p - p_h) \cdot \nabla q_h &= \left(- \left[c_0 + \frac{\alpha^2}{(2\mu^P + \lambda^P)}\right] \int_{\Omega} pq_h + \frac{\alpha}{2\mu^P + \lambda^P} \int_{\Omega} \phi q_h\right) \\ &\quad + \left(\frac{\rho}{\xi} \int_{\Omega} \kappa \mathbf{g} \cdot \nabla q_h + \int_{\Omega} sq\right) - \int_{\Omega} (\kappa/\xi) \nabla p_h \cdot \nabla q_h \end{aligned}$$

for all $q_h \in V_h$. We can next apply integration by parts and choose $q_h = \zeta_e$. Then, from (3.8) we arrive at

$$\begin{aligned} \rho_2 \|R_e\|_{0,e}^2 &\lesssim \sum_{K \in P_e} \int_K R_4 \zeta_e + \sum_{K \in P_e} \int_K (\kappa/\xi) \nabla(p - p_h) \cdot \nabla \zeta_e + \sum_{K \in P_e} \int_K (s^P - s_h^P) \zeta_e \\ &\quad - \left(c_0 + \frac{\alpha^2}{(2\mu^P + \lambda^P)} \right) \sum_{K \in P_e} \int_K (p - p_h) \zeta_e + \frac{\alpha}{2\mu^P + \lambda^P} \sum_{K \in P_e} \int_K (\phi - \phi_h) \zeta_e. \end{aligned}$$

And the proof is completed after applying the Cauchy–Schwarz inequality. \square

THEOREM 3.3 (efficiency estimate for the Biot problem). *Let $(\mathbf{u}, \boldsymbol{\omega}, \phi, p)$ and $(\mathbf{u}_h, \boldsymbol{\omega}_h, \phi_h, p_h)$ be the solutions to the formulations (3.2) and (3.5) (or (3.6)), respectively. Then the following efficiency bound holds:*

$$\Psi \leq C_{\text{eff}}(\|(\mathbf{u} - \mathbf{u}_h, \boldsymbol{\omega} - \boldsymbol{\omega}_h, \phi - \phi_h, p - p_h)\| + \widehat{\Upsilon}),$$

where $C_{\text{eff}} > 0$ is a constant independent of mesh size and model parameters.

Proof. The proof is a direct consequence of combining Lemmas 3.1–3.6. \square

4. Rotation-based elasticity-poroelasticity interface problem.

4.1. Continuous formulation. Let Ω now be partitioned into nonoverlapping and connected subdomains Ω^E , Ω^P representing zones composed by the nonpay rock (linearly elastic domain) and a reservoir (poroelastic domain), respectively. We focus on the case where the reservoir is completely surrounded by the elastic subdomain, such that the interface $\Sigma = \partial\Omega^P \cap \partial\Omega^E$ coincides with the boundary of the pay zone. We consider that the normal unit vector \mathbf{n} on Σ points from Ω^P to Ω^E . The problem is stated as follows, which is as in [4], except for the particular scaling used herein:

(4.1a)

$$\sqrt{\mu^P} \operatorname{curl} \boldsymbol{\omega}^P + \nabla \phi^P = \mathbf{f}^P \quad \text{in } \Omega^P,$$

(4.1b)

$$\boldsymbol{\omega}^P - \sqrt{\mu^P} \operatorname{curl} \mathbf{u}^P = \mathbf{0} \quad \text{in } \Omega^P,$$

(4.1c)

$$(2\mu^P + \lambda^P)^{-1} \phi^P + \operatorname{div} \mathbf{u}^P - \alpha(2\mu^P + \lambda^P)^{-1} p^P = 0 \quad \text{in } \Omega^P,$$

(4.1d)

$$[c_0 + \alpha^2(\mu^P + \lambda^P)^{-1}] p^P - \alpha(2\mu^P + \lambda^P)^{-1} \phi^P - \frac{1}{\xi} \operatorname{div} [\kappa(\nabla p^P - \rho \mathbf{g})] = s^P \quad \text{in } \Omega^P,$$

(4.1e)

$$\sqrt{\mu^E} \operatorname{curl} \boldsymbol{\omega}^E + \nabla p^E = \mathbf{f}^E \quad \text{in } \Omega^E,$$

(4.1f)

$$\boldsymbol{\omega}^E - \sqrt{\mu^E} \operatorname{curl} \mathbf{u}^E = \mathbf{0} \quad \text{in } \Omega^E,$$

(4.1g)

$$\operatorname{div} \mathbf{u}^E + (2\mu^E + \lambda^E)^{-1} p^E = 0 \quad \text{in } \Omega^E,$$

(4.1h)

$$\mathbf{u}^E = \mathbf{0} \quad \text{on } \Gamma,$$

(4.1i)

$$\mathbf{u}^P = \mathbf{u}^E, \quad \sqrt{\mu^P} \boldsymbol{\omega}^P \times \mathbf{n} + \phi^P \mathbf{n} = \sqrt{\mu^E} \boldsymbol{\omega}^E \times \mathbf{n} + p^E \mathbf{n}, \quad \frac{\kappa}{\xi} (\nabla p^P - \rho \mathbf{g}) \cdot \mathbf{n} = 0 \quad \text{on } \Sigma.$$

The weak formulation of the rotation-based Biot's poroelasticity in Ω^P is as follows:

$$\begin{aligned} & -\sqrt{\mu^P} \int_{\Omega^P} \mathbf{curl} \mathbf{v}^P \cdot \boldsymbol{\omega}^P + \int_{\Omega^P} \phi^P \operatorname{div} \mathbf{v}^P - \langle \sqrt{\mu^E} \boldsymbol{\omega}^E \times \mathbf{n} + p^E \mathbf{n}, \mathbf{v}^P \rangle_\Sigma = - \int_{\Omega^P} \mathbf{f}^P \cdot \mathbf{v}^P, \\ & \cdot \int_{\Omega^P} \boldsymbol{\omega}^P \cdot \boldsymbol{\theta}^P - \sqrt{\mu^E} \int_{\Omega^P} \boldsymbol{\theta}^P \cdot \mathbf{curl} \mathbf{u}^P = 0, \\ & \cdot (2\mu^P + \lambda^P)^{-1} \int_{\Omega^P} \phi^P \psi^P + \int_{\Omega^P} \psi^P \operatorname{div} \mathbf{u}^P - \alpha(2\mu^P + \lambda^P)^{-1} \int_{\Omega^P} p^P \psi^P = 0, \\ & - \left[c_0 + \frac{\alpha^2}{(2\mu^P + \lambda^P)} \right] \int_{\Omega^P} p^P q^P + \frac{\alpha}{2\mu^P + \lambda^P} \int_{\Omega^P} \phi^P q^P - \int_{\Omega^P} \frac{\kappa}{\xi} \nabla p^P \cdot \nabla q^P \\ & = - \frac{\rho}{\xi} \int_{\Omega^P} \kappa \mathbf{g} \cdot \nabla q^P - \int_{\Omega^P} s^P q^P \end{aligned}$$

for each $(\mathbf{v}^P, \boldsymbol{\theta}^P, \psi^P, q^P) \in \mathbf{H}^1(\Omega^P) \times \mathbf{L}^2(\Omega^P) \times L^2(\Omega^P) \times H^1(\Omega^P)$. Similarly, for the equations of linear elasticity in Ω^E we get

$$\begin{aligned} & -\sqrt{\mu^E} \int_{\Omega^E} \mathbf{curl} \mathbf{v}^E \cdot \boldsymbol{\omega}^E + \int_{\Omega^E} p^E \operatorname{div} \mathbf{v}^E + \langle \sqrt{\mu^E} \boldsymbol{\omega}^E \times \mathbf{n} + p^E \mathbf{n}, \mathbf{v}^E \rangle_\Sigma = - \int_{\Omega^E} \mathbf{f}^E \cdot \mathbf{v}^E, \\ & \int_{\Omega^E} \boldsymbol{\omega}^E \cdot \boldsymbol{\theta}^E - \sqrt{\mu^E} \int_{\Omega^E} \boldsymbol{\theta}^E \cdot \mathbf{curl} \mathbf{u}^E = 0, \\ & \int_{\Omega} \operatorname{div} \mathbf{u}^E q^E + (2\mu^E + \lambda^E)^{-1} \int_{\Omega^E} p^E q^E = 0 \end{aligned}$$

for each $(\mathbf{v}^E, \boldsymbol{\theta}^E, q^E) \in \mathbf{H}_\Gamma^1(\Omega^E) \times \mathbf{L}^2(\Omega^E) \times L^2(\Omega^E)$, where $\mathbf{H}_\Gamma^1(\Omega^E) = \{\mathbf{v} \in \mathbf{H}^1(\Omega^E) : \mathbf{v}^E = \mathbf{0} \text{ on } \Gamma\}$. We define $\vec{\boldsymbol{\omega}} := \{\boldsymbol{\omega}^P, \phi^P, \boldsymbol{\omega}^E, p^E\}$ and write the weak formulation: find $(\vec{\boldsymbol{\omega}}, \mathbf{u}, p^P) \in \mathbf{H} \times \mathbf{V} \times Q^P$ such that

$$\begin{aligned} a(\vec{\boldsymbol{\omega}}, \vec{\boldsymbol{\theta}}) + b_1(\vec{\boldsymbol{\theta}}, \mathbf{u}) - b_2(\vec{\boldsymbol{\theta}}, p^P) &= 0 & \forall \vec{\boldsymbol{\theta}} \in \mathbf{H}, \\ b_1(\vec{\boldsymbol{\omega}}, \mathbf{v}) &= F(\mathbf{v}) & \forall \mathbf{v} \in \mathbf{V}, \\ b_3(\vec{\boldsymbol{\omega}}, q^P) - c(p^P, q^P) &= G(q^P) & \forall q \in Q^P, \end{aligned}$$

where $\vec{\boldsymbol{\theta}} := (\boldsymbol{\theta}^P, \psi^P, \boldsymbol{\theta}^E, q^E)$. We define spaces as

$$\mathbf{H} := \mathbf{L}^2(\Omega^P) \times \mathbf{L}^2(\Omega^P) \times \mathbf{L}^2(\Omega^E) \times \mathbf{L}^2(\Omega^E), \quad \mathbf{V} := \mathbf{H}_0^1(\Omega), \quad Q^P := H^1(\Omega^P),$$

and the bilinear forms $a : \mathbf{H} \times \mathbf{H} \rightarrow \mathbb{R}$, $b_1 : \mathbf{H} \times \mathbf{V} \rightarrow \mathbb{R}$, $b_2 : \mathbf{H} \times Q^P \rightarrow \mathbb{R}$, $b_3 : \mathbf{H} \times Q^P \rightarrow \mathbb{R}$, $c : Q^P \times Q^P \rightarrow \mathbb{R}$, and linear functionals $F : \mathbf{V} \rightarrow \mathbb{R}$, $G : Q^P \rightarrow \mathbb{R}$ are specified in the following way:

$$\begin{aligned} a(\vec{\boldsymbol{\omega}}, \vec{\boldsymbol{\theta}}) &:= \int_{\Omega^P} \boldsymbol{\omega}^P \cdot \boldsymbol{\theta}^P + \frac{1}{2\mu^P + \lambda^P} \int_{\Omega^P} \phi^P \psi^P + \int_{\Omega^E} \boldsymbol{\omega}^E \cdot \boldsymbol{\theta}^E + \frac{1}{2\mu^E + \lambda^E} \int_{\Omega^E} p^E q^E, \\ b_1(\vec{\boldsymbol{\theta}}, \mathbf{v}) &:= -\sqrt{\mu^P} \int_{\Omega^P} \boldsymbol{\theta}^P \cdot \mathbf{curl} \mathbf{v} + \int_{\Omega^P} \psi^P \operatorname{div} \mathbf{v} - \sqrt{\mu^E} \int_{\Omega^E} \boldsymbol{\theta}^E \cdot \mathbf{curl} \mathbf{v} + \int_{\Omega^E} p^E \operatorname{div} \mathbf{v}, \\ b_2(\vec{\boldsymbol{\theta}}, p^P) &:= \frac{\alpha}{(\lambda^P + 2\mu^P)} \int_{\Omega^P} p^P \psi^P, \quad b_3(\vec{\boldsymbol{\omega}}, q^P) := \frac{\alpha}{(2\mu^P + \lambda^P)} \int_{\Omega^P} q^P \phi^P, \\ c(p^P, q^P) &:= \left[c_0 + \frac{\alpha^2}{(2\mu^P + \lambda^P)} \right] \int_{\Omega^P} p^P q^P + \frac{1}{\xi} \int_{\Omega^P} \kappa \nabla p^P \cdot \nabla q^P, \end{aligned}$$

$$F(\mathbf{v}) := - \int_{\Omega^P} \mathbf{f}^P \cdot \mathbf{v} - \int_{\Omega^E} \mathbf{f}^E \cdot \mathbf{v}, \quad G(q^P) := -\frac{\rho}{\xi} \int_{\Omega^P} \kappa \mathbf{g} \cdot \nabla q^P - \int_{\Omega^P} s^P q^P.$$

For the forthcoming analysis, we will consider the following (μ^E, μ^P) -dependent norm (see, for instance, [25, Remark 2.7] for the case of a single-physics domain) for the displacements:

$$\|\mathbf{v}\|_{\mathbf{V}}^2 := \mu^P \|\mathbf{curl} \mathbf{v}\|_{0,\Omega^P}^2 + \mu^P \|\operatorname{div} \mathbf{v}\|_{0,\Omega^P}^2 + \mu^E \|\mathbf{curl} \mathbf{v}\|_{0,\Omega^E}^2 + \mu^E \|\operatorname{div} \mathbf{v}\|_{0,\Omega^E}^2,$$

and \mathbf{H} will be endowed with the norm

$$\begin{aligned} \|\vec{\boldsymbol{\theta}}\|_{\mathbf{H}}^2 &:= \|\boldsymbol{\theta}^P\|_{0,\Omega^P}^2 + \frac{1}{\mu^P} \|\psi_0^P\|_{0,\Omega^P}^2 + \frac{1}{2\mu^P + \lambda^P} \|\psi^P\|_{0,\Omega^P}^2 + \|\boldsymbol{\theta}^E\|_{0,\Omega^E}^2 \\ &\quad + \frac{1}{\mu^E} \|q_0^E\|_{0,\Omega^E}^2 + \frac{1}{2\mu^E + \lambda^E} \|q^E\|_{0,\Omega^E}^2. \end{aligned}$$

Now, we write down the compact form of the weak formulation as follows:

$$(4.2) \quad B_I((\vec{\boldsymbol{\omega}}, \mathbf{u}, p^P), (\vec{\boldsymbol{\theta}}, \mathbf{v}, q^P)) = F(\mathbf{v}) + G(q^P),$$

where the multilinear form now has a subscript I (for *interface* problem), and it is defined as

$$\begin{aligned} B_I((\vec{\boldsymbol{\omega}}, \mathbf{u}, p^P), (\vec{\boldsymbol{\theta}}, \mathbf{v}, q^P)) &:= a(\vec{\boldsymbol{\omega}}, \vec{\boldsymbol{\theta}}) + b_1(\vec{\boldsymbol{\theta}}, \mathbf{u}) - b_2(\vec{\boldsymbol{\theta}}, p^P) \\ &\quad + b_1(\vec{\boldsymbol{\omega}}, \mathbf{v}) + b_3(\vec{\boldsymbol{\omega}}, q^P) - c(p^P, q^P). \end{aligned}$$

We now turn our attention to the stability estimates. The following theorem will also be very useful in the forthcoming analysis.

THEOREM 4.1. *Assume $\frac{\alpha^2}{2\mu^P + \lambda^P} \in (0, 9c_0/10]$. For every $(\vec{\boldsymbol{\omega}}, \mathbf{u}, p^P) \in \mathbf{H} \times \mathbf{V} \times Q^P$, there exists $(\vec{\boldsymbol{\theta}}, \mathbf{v}, q^P) \in \mathbf{H} \times \mathbf{V} \times Q^P$ with $\|(\vec{\boldsymbol{\theta}}, \mathbf{v}, q^P)\| \leq C_1 \|(\vec{\boldsymbol{\omega}}, \mathbf{u}, p^P)\|$ such that*

$$B_I((\vec{\boldsymbol{\omega}}, \mathbf{u}, p^P), (\vec{\boldsymbol{\theta}}, \mathbf{v}, q^P)) \geq C_2 \|(\vec{\boldsymbol{\omega}}, \mathbf{u}, p^P)\|^2,$$

where $\|(\vec{\boldsymbol{\theta}}, \mathbf{v}, q^P)\|^2 := \|\mathbf{v}\|_{\mathbf{V}}^2 + \|\vec{\boldsymbol{\theta}}\|_{\mathbf{H}}^2 + (c_0 + \frac{\alpha^2}{(2\mu^P + \lambda^P)}) \|q^P\|_{0,\Omega^P}^2 + \|\kappa/\xi(\nabla q^P)\|_{0,\Omega^P}^2$.

Proof. Invoking the relevant inf-sup condition, for each $p^E \in L^2(\Omega^E)$ and $\phi^P \in L^2(\Omega^P)$, we can find $\mathbf{v}_0^E \in \mathbf{H}_0^1(\Omega^E)$ and $\mathbf{v}_0^P \in \mathbf{H}_0^1(\Omega^P)$ such that

$$\begin{aligned} (\operatorname{div} \mathbf{v}_0^E, p^E)_{0,\Omega^E} &\geq C_{\Omega^E}/\mu^E \|p_0^E\|_{0,\Omega^E}^2, \quad \sqrt{\mu^E} \|\nabla \mathbf{v}_0^E\|_{0,\Omega^E} \leq 1/\sqrt{\mu^E} \|p_0^E\|_{0,\Omega^E}, \\ (\operatorname{div} \mathbf{v}_0^P, \phi^P)_{0,\Omega^P} &\geq C_{\Omega^P}/\mu^P \|\phi_0^P\|_{0,\Omega^P}^2, \quad \sqrt{\mu^P} \|\nabla \mathbf{v}_0^P\|_{0,\Omega^P} \leq 1/\sqrt{\mu^P} \|\phi_0^P\|_{0,\Omega^P}. \end{aligned}$$

Hence, for $\mathbf{v}_0 \in \mathbf{H}_0^1(\Omega)$ such that $\mathbf{v}_0|_{\Omega^E} = \mathbf{v}_0^E$ and $\mathbf{v}_0|_{\Omega^P} = \mathbf{v}_0^P$, we have

$$\begin{aligned} B_I((\vec{\boldsymbol{\omega}}, \mathbf{u}, p^P), (\mathbf{0}, \mathbf{v}_0, 0)) &= -\sqrt{\mu^P} \int_{\Omega^P} \boldsymbol{\omega}^P \cdot \mathbf{curl} \mathbf{v}_0^P + \int_{\Omega^P} \phi^P \operatorname{div} \mathbf{v}_0^P \\ &\quad - \sqrt{\mu^E} \int_{\Omega^E} \boldsymbol{\omega}^E \cdot \mathbf{curl} \mathbf{v}_0^E + \int_{\Omega^E} p^E \operatorname{div} \mathbf{v}_0 \geq \left(C_{\Omega^P} - \frac{1}{2\epsilon_1} \right) \frac{1}{\mu^P} \|\phi_0^P\|_{0,\Omega^P}^2 \\ &\quad + \left(C_{\Omega^E} - \frac{1}{2\epsilon_2} \right) \frac{1}{\mu^E} \|p_0^E\|_{0,\Omega^E}^2 - \frac{\epsilon_2}{2} \|\boldsymbol{\omega}^E\|_{0,\Omega^E} - \frac{\epsilon_1}{2} \|\boldsymbol{\omega}^P\|_{0,\Omega^P}. \end{aligned}$$

Selecting $\vec{\theta} = \vec{\omega}$, $\mathbf{v} = -\mathbf{u}$, and $q^P = -p^P$ we have

$$\begin{aligned} B_I((\vec{\omega}, \mathbf{u}, p^P), (\vec{\omega}, -\mathbf{u}, -p^P)) &= \|\omega^E\|_{0,\Omega^E}^2 + (2\mu^E + \lambda^E)^{-1} \|p^E\|_{0,\Omega^E}^2 \\ &\quad + \|\omega^P\|_{0,\Omega^P}^2 + (2\mu^P + \lambda^P)^{-1} \|\phi^P\|_{0,\Omega^P}^2 \\ &\quad - 2\alpha(2\mu^P + \lambda^P)^{-1} (p^P, \phi^P)_{0,\Omega^P} + (c_0 + \alpha^2(2\mu^P + \lambda^P)^{-1}) \|p^P\|_{0,\Omega^P}^2 \\ &\quad + \|(\kappa/\xi)^{1/2} \nabla p\|_{0,\Omega^P}^2. \end{aligned}$$

Next, we take $\vec{\theta}_1 := (-\sqrt{\mu^P} \operatorname{curl} \mathbf{u}^P, \mu^P \operatorname{div} \mathbf{u}^P, -\sqrt{\mu^E} \operatorname{curl} \mathbf{u}^E, \mu^E \operatorname{div} \mathbf{u}^E) \in \mathbf{H}$, $\mathbf{v} = \mathbf{0}$, and $q^P = 0$. Then

$$\begin{aligned} &B_I((\vec{\omega}, \mathbf{u}, p^P), (\vec{\theta}_1, \mathbf{0}, 0)) \\ &= \mu^E \|\operatorname{curl} \mathbf{u}^E\|_{0,\Omega^E}^2 + \mu^E \|\operatorname{div} \mathbf{u}^E\|_{0,\Omega^E}^2 - \sqrt{\mu^E} (\omega^E, \operatorname{curl} \mathbf{u}^E)_{0,\Omega^E} \\ &\quad + \mu^E / (2\mu^E + \lambda^E) (p^E, \operatorname{div} \mathbf{u}^E)_{0,\Omega^E} \\ &\quad + \mu^P \|\operatorname{curl} \mathbf{u}^P\|_{0,\Omega^P}^2 + \mu^P \|\operatorname{div} \mathbf{u}^P\|_{0,\Omega^P}^2 - \sqrt{\mu^P} (\omega^P, \operatorname{curl} \mathbf{u}^P)_{0,\Omega^P} \\ &\quad + \mu^P (2\mu^P + \lambda^P)^{-1} (\phi^P, \operatorname{div} \mathbf{u}^P)_{0,\Omega^P} - \alpha \mu^P (2\mu^P + \lambda^P)^{-1} (p^P, \operatorname{div} \mathbf{u}^P)_{0,\Omega^P} \\ &\geq \frac{\mu^P}{2} \|\operatorname{curl} \mathbf{u}^P\|_{0,\Omega^P}^2 + \left(1 - \frac{\mu^P}{(2\mu^P + \lambda^P)}\right) \mu^P \|\operatorname{div} \mathbf{u}^P\|_{0,\Omega^P}^2 \\ &\quad - \frac{1}{2} \|\omega^P\|_{0,\Omega^P}^2 - \frac{\alpha^2}{2(2\mu^P + \lambda^P)} \|p^P\|_{0,\Omega^P}^2 - \frac{1}{2(2\mu^P + \lambda^P)} \|\phi^P\|_{0,\Omega^P}^2 + \frac{\mu^E}{2} \|\operatorname{curl} \mathbf{u}^E\|^2 \\ &\quad + \frac{\mu^E}{2} \|\operatorname{div} \mathbf{u}^E\|_{0,\Omega^E}^2 - \frac{1}{2} \|\omega^E\|_{0,\Omega^E}^2 - \frac{\mu^E}{2(2\mu^E + \lambda^E)^2} \|p^E\|_{0,\Omega^E}^2. \end{aligned}$$

Then we can make the choices $\mathbf{v} = -\mathbf{u} + \delta_1 \mathbf{v}_0$, $\vec{\theta} = \vec{\omega} + \delta_2 \vec{\theta}_1$, and $q^P = -p^P$, leading to

$$\begin{aligned} &B_I((\vec{\omega}, \mathbf{u}, p^P), (\vec{\omega} + \delta_2 \vec{\theta}_1, -\mathbf{u} + \delta_1 \mathbf{v}_0, -p^P)) \\ &= B_I((\vec{\omega}, \mathbf{u}, p^P), (\vec{\omega}, -\mathbf{u}, -p^P)) + \delta_1 B_I((\vec{\omega}, \mathbf{u}, p^P), (\mathbf{0}, \mathbf{v}_0, 0)) \\ &\quad + \delta_2 B_I((\vec{\omega}, \mathbf{u}, p^P), (\vec{\theta}_1, \mathbf{0}, 0)) \geq \left(1 - \frac{\delta_1 \epsilon_2}{2} - \frac{\delta_2}{2}\right) \|\omega^E\|_{0,\Omega^E}^2 + \delta_2 \frac{\mu^E}{2} \|\operatorname{curl} \mathbf{u}^E\|_{0,\Omega^E}^2 \\ &\quad + \delta_2 \frac{\mu^E}{2} \|\operatorname{div} \mathbf{u}^E\|_{0,\Omega^E}^2 + \delta_1 \left(C_{\Omega^E} - \frac{1}{2\epsilon_2}\right) \frac{1}{\mu^E} \|p_0^E\|_{0,\Omega^E}^2 \\ &\quad + \frac{1}{2\mu^E + \lambda^E} \left(1 - \frac{\delta_2 \mu^E}{2\mu^E + \lambda^E}\right) \|p^E\|_{0,\Omega^E}^2 + \left(1 - \frac{\delta_1 \epsilon_1}{2} - \frac{\delta_2}{2}\right) \|\omega^P\|_{0,\Omega^P}^2 \\ &\quad + \frac{\mu^P \delta_2}{2} \|\operatorname{curl} \mathbf{u}^P\|_{0,\Omega^P}^2 + \delta_1 \left(1 - \frac{\mu^P}{(2\mu^P + \lambda^P)}\right) \|\operatorname{div} \mathbf{u}^P\|_{0,\Omega^P}^2 \\ &\quad + \left(C_{\Omega^P} - \frac{1}{2\epsilon_2}\right) \frac{\delta_1}{\mu^P} \|\phi_0^P\|_{0,\Omega^P}^2 + \frac{1}{2\mu^P + \lambda^P} \left(\frac{1}{2} - \frac{\delta_2}{2}\right) \|\phi^P\|_{0,\Omega^P}^2 \\ &\quad + \|(\kappa/\xi)^{1/2} \nabla p^P\|_{0,\Omega^P}^2 + \left(c_0 + \frac{\alpha^2}{(2\mu^P + \lambda^P)} \left(-1 - \frac{\delta_2}{2}\right)\right) \|p^P\|_{0,\Omega^P}^2. \end{aligned}$$

Assuming the values $\epsilon_1 = \epsilon_2 = \min\{1/C_{\Omega^E}, 1/C_{\Omega^P}\}$, $\delta_1 = 1/2\epsilon_1$, and $\delta_2 = 1/5$, we then have

$$B_I((\vec{\omega}, \mathbf{u}, p^P), (\vec{\theta}, \mathbf{v}, q^P)) \geq \frac{1}{4} \min \left\{ \min \{C_{\Omega^E}^2, C_{\Omega^P}^2\}, \frac{1}{50} \right\} \|(\vec{\omega}, \mathbf{u}, p^P)\|^2.$$

Finally, the proof concludes after realizing that

$$\|(\vec{\theta}, \mathbf{v}, q^P)\|^2 = \|(\vec{\omega} + \delta_2 \vec{\theta}_1, -\mathbf{u} + \delta_1 \mathbf{v}_0, -p^P)\|^2 \leq 2 \|(\vec{\omega}, \mathbf{u}, p^P)\|^2. \quad \square$$

4.2. Discrete spaces and Galerkin formulation. Let $\{\mathcal{T}_h\}_{h>0}$ be a shape-regular family of partitions of the closed domain $\bar{\Omega}$, conformed by tetrahedra (or triangles in 2D) K of diameter h_K , with mesh size $h := \max\{h_K : K \in \mathcal{T}_h\}$. In addition, we assume that the mesh is conforming with the interface. This is achieved, for example, by generating conforming simplicial meshes for Ω^P and for Ω^E and requiring that they match on Σ so that the union of the subdomain meshes is a triangulation of $\Omega^P \cup \Sigma \cup \Omega^E$. We specify the finite-dimensional subspaces for displacement, fluid pressure, rotations, and total pressure as follows:

$$\begin{aligned} \mathbf{V}_h &:= \{\mathbf{v}_h \in \mathbf{C}(\bar{\Omega}) \cap \mathbf{V} : \mathbf{v}_h|_K \in \mathbb{P}_{k+1}(K)^d \ \forall K \in \mathcal{T}_h\}, \\ Q_h^P &:= \{q_h^P \in \mathbf{C}(\bar{\Omega}^P) : q_h^P|_K \in \mathbb{P}_{k+1}(K) \ \forall K \in \mathcal{T}_h\}, \\ \mathbf{W}_h^P &:= \{\boldsymbol{\theta}_h^P \in \mathbf{L}^2(\Omega^P) : \boldsymbol{\theta}_h^P|_K \in \mathbb{P}_k(K)^{d(d-1)/2} \ \forall K \in \mathcal{T}_h\}, \\ \mathbf{W}_h^E &:= \{\boldsymbol{\theta}_h^E \in \mathbf{L}^2(\Omega^E) : \boldsymbol{\theta}_h^E|_K \in \mathbb{P}_k(K)^{d(d-1)/2} \ \forall K \in \mathcal{T}_h\}, \\ Z_h^P &:= \{\psi_h^P \in \mathbf{L}^2(\Omega^P) : \psi_h^P|_K \in \mathbb{P}_k(K) \ \forall K \in \mathcal{T}_h\}, \\ Z_h^E &:= \{q_h^E \in \mathbf{L}^2(\Omega^E) : q_h^E|_K \in \mathbb{P}_k(K) \ \forall K \in \mathcal{T}_h\}. \end{aligned}$$

Define $\vec{\omega}_h := \{\omega_h^P, \phi_h^P, \omega_h^E, p_h^E\} \in \mathbf{W}_h^P \times Z_h^P \times \mathbf{W}_h^E \times Z_h^E := \mathbf{H}_h$. The discrete weak formulation of the rotation based elasticity is read as follows: find $(\vec{\omega}_h, \mathbf{u}_h, p_h^P) \in \mathbf{H}_h \times \mathbf{V}_h \times Q_h^P$ such that

$$(4.3) \quad B_I((\vec{\omega}_h, \mathbf{u}_h, p_h^P), (\vec{\theta}, \mathbf{v}, q^P)) = F(\mathbf{v}) + G(q)$$

for all $(\vec{\theta}, \mathbf{v}, q^P) \in \mathbf{H}_h \times \mathbf{V}_h \times Q_h^P$. For each $k \geq 0$, the modified (stabilized) discrete weak formulation of the rotation based elasticity reads as follows: find $(\vec{\omega}_h, \mathbf{u}_h, p_h^P) \in \mathbf{H}_h \times \mathbf{V}_h \times Q_h^P$ such that

$$(4.4) \quad \begin{aligned} B_I((\vec{\omega}_h, \mathbf{u}_h, p_h^P), (\vec{\theta}, \mathbf{v}, q^P)) + \sum_{e \in \mathcal{E}(\mathcal{T}_h) \cap \Omega^E} \frac{h_e}{\mu^E} \int_e [\![p_h^E]\!] [\!q^E]\!] \\ + \sum_{e \in \mathcal{E}(\mathcal{T}_h) \cap \Omega^P} \frac{h_e}{\mu^P} \int_e [\![\phi_h^P]\!] [\!\psi^P]\!] = F(\mathbf{v}) + G(q) \end{aligned}$$

for all $(\vec{\theta}, \mathbf{v}, q^P) \in \mathbf{H}_h \times \mathbf{V}_h \times Q_h^P$.

4.3. A posteriori error analysis. Let Θ_K^2 , Ψ_K^2 , and Λ_e^2 be the elasticity estimator (cf. (2.5)), the poroelasticity estimator (cf. (3.7)), and the interface estimator (see below), respectively. Then we define

$$\Xi^2 := \sum_{K \in \mathcal{T}_h \cap \Omega^E} \Theta_K^2 + \sum_{K \in \mathcal{T}_h \cap \Omega^P} \Psi_K^2 + \sum_{e \in \mathcal{E}(\mathcal{T}_h) \cap \Sigma} \Lambda_e^2,$$

where

$$\Lambda_e^2 := h_e(\mu^E + \mu^P)^{-1} \|\mathbf{R}_\Sigma\|_{0,e}^2 + h_e \xi \kappa^{-1} \|\widehat{\mathbf{R}}_\Sigma\|_{0,e}^2,$$

and

$$\mathbf{R}_\Sigma := \{\sqrt{\mu^P} \omega_h^P \times \mathbf{n} + \phi_h^P \mathbf{n} - \sqrt{\mu^E} \omega_h^E \times \mathbf{n} - p_h^E \mathbf{n}\}, \quad \widehat{\mathbf{R}}_\Sigma := \{\kappa \xi^{-1} (\nabla p_h^P - \rho \mathbf{g}) \cdot \mathbf{n}\}.$$

Next, we define the global data oscillations term Υ as

$$\Upsilon^2 := \sum_{K \in \mathcal{T}_h \cap \Omega^E} \tilde{\Upsilon}_K^2 + \sum_{K \in \mathcal{T}_h \cap \Omega^P} \hat{\Upsilon}_K^2,$$

where $\tilde{\Upsilon}_K$ and $\hat{\Upsilon}_K$ are the local data oscillations for elasticity and poroelasticity, respectively.

4.3.1. Reliability estimate. In this section, we prove the reliability bound for the interface estimator.

THEOREM 4.2 (reliability for the transmission problem). *Let $(\vec{\omega}, \mathbf{u}, p^P)$ and $(\vec{\omega}_h, \mathbf{u}_h, p_h^P)$ be the solutions of the weak formulations (4.2) and (4.3) (or (4.4)), respectively. Then the following reliability bound holds:*

$$\|(\vec{\omega} - \vec{\omega}_h, \mathbf{u} - \mathbf{u}_h, p^P - p_h^P)\| \leq C_{\text{rel}}(\Xi + \Upsilon),$$

where $C_{\text{rel}} > 0$ is a positive constant independent of mesh size and parameters.

Proof. Since $(\vec{\omega} - \vec{\omega}_h, \mathbf{u} - \mathbf{u}_h, p^P - p_h^P) \in \mathbf{H} \times \mathbf{V} \times Q^P$, then from the stability theorem we have

$$C_2 \|(\vec{\omega} - \vec{\omega}_h, \mathbf{u} - \mathbf{u}_h, p^P - p_h^P)\|^2 \leq B_I((\vec{\omega} - \vec{\omega}_h, \mathbf{u} - \mathbf{u}_h, p^P - p_h^P), (\vec{\theta}, \mathbf{v}, q^P)),$$

with $\|(\vec{\theta}, \mathbf{v}, q^P)\| \leq C_1 \|(\vec{\omega} - \vec{\omega}_h, \mathbf{u} - \mathbf{u}_h, p^P - p_h^P)\|$. And from the definition of the continuous and discrete weak forms, it follows that

$$\begin{aligned} & B_I((\vec{\omega} - \vec{\omega}_h, \mathbf{u} - \mathbf{u}_h, p^P - p_h^P), (\vec{\theta}, \mathbf{v}, q^P)) \\ &= -(\mathbf{f}^P - \mathbf{f}_h^P, \mathbf{v} - \mathbf{v}_h)_{0, \Omega^P} - (\mathbf{f}^E - \mathbf{f}_h^E, \mathbf{v} - \mathbf{v}_h)_{0, \Omega^E} - \frac{\rho}{\xi} (\kappa \mathbf{g}, \nabla(q - q_h))_{0, \Omega^P} \\ &+ (s^P - s_h^P, q - q_h)_{0, \Omega^P} - (\mathbf{f}_h^P, \mathbf{v} - \mathbf{v}_h)_{0, \Omega^P} - (\mathbf{f}_h^E, \mathbf{v} - \mathbf{v}_h)_{0, \Omega^E} + (s_h^P, q - q_h)_{0, \Omega^P} \\ &- B_I((\vec{\omega}_h, \mathbf{u}_h, p_h^P), (\vec{\theta}, \mathbf{v} - \mathbf{v}_h, q^P - q_h^P)). \end{aligned}$$

Applying integration by parts, the Cauchy–Schwarz inequality, and approximation results yields

$$B_I((\vec{\omega} - \vec{\omega}_h, \mathbf{u} - \mathbf{u}_h, p^P - p_h^P), (\vec{\theta}, \mathbf{v}, q^P)) \leq C(\Xi + \Upsilon) \|(\vec{\theta}, \mathbf{v}, q^P)\|. \quad \square$$

4.3.2. Efficiency bound.

LEMMA 4.1. *The following estimates are satisfied:*

$$\Theta \lesssim \|(\vec{\omega} - \vec{\omega}_h, \mathbf{u} - \mathbf{u}_h, p^P - p_h^P)\| + \Upsilon, \quad \Psi \lesssim \|(\vec{\omega} - \vec{\omega}_h, \mathbf{u} - \mathbf{u}_h, p^P - p_h^P)\| + \Upsilon.$$

Proof. The first bound follows from Theorem 3.3, while the second one follows from Theorem 2.3. \square

LEMMA 4.2. *The following holds:*

$$\begin{aligned} & \left(\sum_{e \in \Sigma} h_e (\mu^E + \mu^P)^{-1} \|\mathbf{R}_\Sigma\|_{0,e}^2 \right)^{1/2} \lesssim \sum_{e \in \Sigma} \left(\sum_{K \in P_e \cap \Omega^E} ((\mu^E)^{-1/2} h_K \|\mathbf{f}^E - \mathbf{f}_h^E\|_{0,K} \right. \\ &+ (\mu^E)^{-1/2} \|p^E - p_h^E\|_{0,K} + \|\omega^E - \omega_h^E\|_{0,K}) + \sum_{K \in P_e \cap \Omega^P} ((\mu^P)^{-1/2} h_K \|\mathbf{f}^P - \mathbf{f}_h^P\|_{0,K} \\ &+ (\mu^P)^{-1/2} \|\phi^P - \phi_h^P\|_{0,K} + \|\omega^P - \omega_h^P\|_{0,K}) \Big). \end{aligned}$$

Proof. For each $e \in \mathcal{E}(\mathcal{T}_h) \cap \Sigma$, we locally define $\zeta_e = (\mu^E + \mu^P)^{-1} h_e \mathbf{R}_\Sigma b_e$. Using (2.9) implies

$$h_e(\mu^E + \mu^P)^{-1} \|\mathbf{R}_\Sigma\|_{0,e}^2 \lesssim \int_e \mathbf{R}_\Sigma \cdot ((\mu^E + \mu^P)^{-1} h_e \mathbf{R}_\Sigma b_e) = \int_e \mathbf{R}_\Sigma \cdot \zeta_e.$$

Integration by parts gives

$$\begin{aligned} & \int_e \sqrt{\mu^E} (\omega_h^E - \omega^E) \times \mathbf{n} + (p_h^E - p^E) \mathbf{n} \cdot \zeta_e - \sqrt{\mu^P} (\omega_h^P - \omega^P) \times \mathbf{n} + (\phi_h^P - \phi^P) \mathbf{n} \cdot \zeta_e \\ &= \sum_{K \in P_e \cap \Omega^E} \int_K (\sqrt{\mu^E} \operatorname{curl}(\omega_h^E - \omega^E) + \nabla(p_h^E - p^E) \cdot \zeta_e) \\ &+ \sum_{K \in P_e \cap \Omega^P} \int_K (\sqrt{\mu^E} (\omega_h^E - \omega^E) \cdot \operatorname{curl} \zeta_e + (p_h^E - p^E) \operatorname{div} \nabla \cdot \zeta_e) \\ &+ \sum_{K \in P_e \cap \Omega^P} \int_K (\sqrt{\mu^P} \operatorname{curl}(\omega_h^P - \omega^P) + \nabla(\phi_h^P - \phi^P) \cdot \zeta_e) \\ &+ \sum_{K \in P_e \cap \Omega^P} \int_K (\sqrt{\mu^P} (\omega_h^P - \omega^P) \cdot \operatorname{curl} \zeta_e + (\phi_h^P - \phi^P) \operatorname{div} \nabla \cdot \zeta_e). \end{aligned}$$

Recall that $\mathbf{f}^P - \sqrt{\mu^P} \operatorname{curl} \omega^P - \nabla p^P = \mathbf{0}|_K$ and $\mathbf{f}^E - \sqrt{\mu^E} \operatorname{curl} \omega^E - \nabla p^E = \mathbf{0}|_K$. Then, we have

$$\begin{aligned} \frac{h_e}{\mu^E + \mu^P} \|\mathbf{R}_\Sigma\|_{0,e}^2 &\lesssim \sum_{K \in P_e \cap \Omega^E} \int_K \left((\mathbf{f}_h^E - \mathbf{f}^E) \cdot \zeta_e + \sqrt{\mu^E} \int_K (\omega_h^E - \omega^E) \cdot \operatorname{curl} \zeta_e \right. \\ &\quad \left. + \int_K (p_h^E - p^E) \operatorname{div} \nabla \cdot \zeta \right) \\ &+ \sum_{K \in P_e \cap \Omega^E} \int_K \mathbf{R}_1^E \cdot \zeta_e + \sum_{K \in P_e \cap \Omega^P} \int_K \mathbf{R}_1^P \cdot \zeta_e \\ &+ \sum_{K \in P_e \cap \Omega^P} \int_K \left((\mathbf{f}_h^P - \mathbf{f}^P) \cdot \zeta_e + \sqrt{\mu^P} \int_K (\omega_h^P - \omega^P) \cdot \operatorname{curl} \zeta_e \right. \\ &\quad \left. + \int_K (\phi_h^P - \phi^P) \operatorname{div} \nabla \cdot \zeta \right). \end{aligned}$$

Next, we can apply the Cauchy–Schwarz inequality, leading to

$$\begin{aligned} \frac{h_e}{\mu^E + \mu^P} \|\mathbf{R}_e\|_{0,e}^2 &\lesssim \sum_{K \in P_e \cap \Omega^E} ((\mu^E)^{-1/2} h_K \|\mathbf{f}^E - \mathbf{f}_h^E\|_{0,K} + (\mu^E)^{-1/2} \|p^E \right. \\ &\quad \left. - p_h^E\|_{0,K} + \|\omega^E - \omega_h^E\|_{0,K}) \times ((\mu^E)^{1/2} \|\nabla \zeta\|_{0,K} + (\mu^E)^{1/2} h_K^{-1} \|\zeta\|_{0,K}) \\ &+ \sum_{K \in P_e \cap \Omega^P} ((\mu^P)^{-1/2} h_K \|\mathbf{f}^P - \mathbf{f}_h^P\|_{0,K} + (\mu^P)^{-1/2} \|\phi^P - \phi_h^P\|_{0,K} \\ &+ \|\omega^P - \omega_h^P\|_{0,K}) \times ((\mu^P)^{1/2} \|\nabla \zeta\|_{0,K} + (\mu^P)^{1/2} h_K^{-1} \|\zeta\|_{0,K}). \end{aligned}$$

The sought estimate is then a consequence of the bounds

$$\begin{aligned} & (\mu^E)^{1/2} \|\nabla \zeta\|_{0,K} + (\mu^E)^{1/2} h_K^{-1} \|\zeta\|_{0,K} \lesssim (\mu^E)^{1/2} h_K^{-1} \|\zeta\|_{0,K} \\ & \lesssim h_e^{1/2} (\mu^E + \mu^P)^{-1/2} \|\mathbf{R}_e\|_{0,e}, \end{aligned}$$

$$\begin{aligned} (\mu^P)^{1/2} \|\nabla \zeta\|_{0,K} + (\mu^P)^{1/2} h_K^{-1} \|\zeta\|_{0,K} &\lesssim (\mu^P)^{1/2} h_K^{-1} \|\zeta\|_{0,K} \\ &\lesssim h_e^{1/2} (\mu^E + \mu^P)^{-1/2} \|\mathbf{R}_e\|_{0,e}. \end{aligned}$$
□

LEMMA 4.3. *The following bound holds:*

$$\left(\sum_{e \in \mathcal{E}(\mathcal{T}_h) \cap \Sigma} \Lambda_e^2 \right)^{1/2} \lesssim \|(\vec{\omega} - \vec{\omega}_h, \mathbf{u} - \mathbf{u}_h, p^P - p_h^P)\| + \Upsilon.$$

Proof. The proof follows straightforwardly from Lemma 3.6. □

THEOREM 4.3 (efficiency estimate). *Let $(\vec{\omega}, \mathbf{u}, p^P)$ and $(\vec{\omega}_h, \mathbf{u}_h, p_h^P)$ be the solutions to (4.2) and (4.3) (or (4.4)), respectively. Then, the following efficiency bound holds:*

$$\Xi \leq C_{\text{eff}} (\|(\vec{\omega} - \vec{\omega}_h, \mathbf{u} - \mathbf{u}_h, p^P - p_h^P)\| + \Upsilon),$$

where $C_{\text{eff}} > 0$ is a constant independent of h and of the sensible model parameters.

Proof. The bound results from combining Lemmas 4.1–4.3. □

5. Computational examples. The accuracy of the three finite element discretizations and the robustness of the corresponding a posteriori error estimators will be demonstrated in this section. As usual, such robustness is quantified in terms of the effectivity index of a given computable indicator $\Phi \in \{\Theta, \Psi, \Xi\}$, i.e., the ratio between the total actual error and the estimated error

$$\mathbf{eff}(\Phi) = (\mathbf{e}_{\mathbf{u}}^2 + \mathbf{e}_p^2 + \dots)^{1/2} / \Phi_K,$$

and \mathbf{eff} is expected to remain constant independently of the number of degrees of freedom associated with each mesh refinement. The direct solver UMFPACK is used for all linear systems, and the algorithms are implemented in the FEniCS library [2], using multiphenics [8] for the handling of subdomains and incorporation of restricted finite element spaces. We emphasize, however, that no splitting algorithms have been implemented for the present formulations. All the methods analyzed in the previous sections are realized using a monolithic approach.

We start with a simple case of manufactured solutions on $\Omega = (0, 1)^2$, where both displacement and fluid pressure vanish on $\partial\Omega$,

$$p(x, y) = xy(1-x)(a-y), \quad \mathbf{u}(x, y) = \begin{pmatrix} \pi \sin^2(\pi x) \sin(\pi y) \cos(\pi y) + p(x, y)/2\lambda \\ -\pi \sin(\pi x) \cos(\pi y) \sin^2(\pi y) + p(x, y)/2\lambda \end{pmatrix}.$$

To ensure the zero boundary condition for displacement, we choose $a = 1$. In the interface problem, we choose $a = 0.5$ for fluid pressure. Unless specified otherwise, all parameters (except the Poisson ratio) are taken equal to 1. For the transmission problem the interface is the horizontal segment located on $y = \frac{1}{2}$, and the porous domain is below the interface. A sequence of successively refined uniform meshes is constructed, and exact and estimated errors between these closed-form solutions and the finite element approximations (in this case focusing on the first- and second-order schemes, with $k = 0$ and $k = 1$) are computed. The results are collected in Tables 5.1, 5.2, and 5.3, where the convergence rates are computed as

$$(5.1) \quad \mathbf{r}_{(\cdot)} = \log(e_{(\cdot)}/\tilde{e}_{(\cdot)}) [\log(h/\tilde{h})]^{-1},$$

where e, \tilde{e} denote errors generated on two consecutive meshes of size h and \tilde{h} .

TABLE 5.1

Example 1A: Errors, convergence rates, and effectivity indexes under uniform mesh refinement. Smooth manufactured solutions for the rotation-based elasticity problem.

DoFs	h	e_{ω}	r_{ω}	e_u	r_u	e	$\text{eff}(\Theta)$
$E = 1, \nu = 0.25, k = 0$							
$E = 1, \nu = 0.25, k = 1$							
114	0.3536	2.14e+0	0.00	2.64e+0	0.00	3.40e+0	0.249
418	0.1768	1.11e+0	0.95	1.40e+0	0.92	1.79e+0	0.248
1602	0.0884	5.61e-01	0.99	7.07e-01	0.98	9.02e-01	0.246
6274	0.0442	2.81e-01	1.00	3.54e-01	1.00	4.52e-01	0.245
24834	0.0221	1.40e-01	1.00	1.77e-01	1.00	2.26e-01	0.244
98818	0.0110	7.02e-02	1.00	8.85e-02	1.00	1.13e-01	0.244
$E = 10^5, \nu = 0.499, k = 0$							
114	0.3536	6.43e+2	0.00	7.24e+2	0.00	9.68e+2	0.222
418	0.1768	3.19e+2	1.01	4.02e+2	0.85	5.14e+2	0.247
1602	0.0884	1.61e+2	0.99	2.04e+2	0.98	2.60e+2	0.245
6274	0.0442	8.08e+1	1.00	1.02e+2	1.00	1.30e+2	0.244
24834	0.0221	4.04e+1	1.00	5.11e+1	1.00	6.51e+1	0.244
98818	0.0110	2.02e+1	1.00	2.55e+1	1.00	3.26e+1	0.244
$E = 10^5, \nu = 0.499, k = 1$							
354	0.3536	2.37e+2	0.00	4.18e+2	0.00	4.81e+2	0.172
1346	0.1768	4.14e+1	2.52	5.94e+1	2.82	7.24e+1	0.150
5250	0.0884	1.06e+1	1.97	1.49e+1	1.99	1.83e+1	0.148
20738	0.0442	2.67e+0	1.99	3.68e+0	2.02	4.55e+0	0.146
82434	0.0221	6.68e-01	2.00	9.17e-01	2.01	1.13e+0	0.146
328706	0.0110	1.67e-01	2.00	2.29e-01	2.00	2.83e-01	0.145

The expected $O(h^{k+1})$ convergence is observed for all fields in their respective norms, in accordance with the theory from [5, 4], and the effectivity index is close to constant for all mesh refinements. This same behavior is seen even when the elastic or the poroelastic material is nearly incompressible (setting $E = 10^5, \nu = 0.499$) and when the poroelastic material is nearly impermeable (setting $\kappa = 10^{-12}$), and we also note that the effectivity index is slightly modified, but it is still constant and not affected by the different parameter scaling, again confirming the robustness of the estimators. The variation in efficiency is not surprising as our analysis only focuses on h -adaptivity based a posteriori error estimation (and an extension to hp -adaptivity based a posteriori error estimators might help to overcome such a variation).

For the second and third examples, we employ adaptive mesh refinement consisting of the usual steps of solving, then computing the local and global estimators, marking, refining, and smoothing. The marking of elements for refinement follows the classical Dörfler approach [18]: a given $K \in \mathcal{T}_h$ is *marked* (added to the marking set $\mathcal{M}_h \subset \mathcal{T}_h$) whenever the local error indicator Φ_K satisfies $\sum_{K \in \mathcal{M}_h} \Phi_K^2 \geq \zeta \sum_{K \in \mathcal{T}_h} \Phi_K^2$, where $0 < \zeta < 1$ is a user-defined parameter (meaning that one refines elements that contribute to a proportion ζ of the total squared error). Elements in \mathcal{M}_h are then refined (their diameter is halved) and an additional smoothing step is applied before starting a new iteration of the algorithm. When computing convergence

TABLE 5.2

Example 1B: Errors (combining rotation and total pressure into $\vec{\omega}$), convergence rates, and effectivity indexes under uniform mesh refinement. Smooth manufactured solutions for the rotation-based Biot problem.

DoFs	h	$e_{\vec{\omega}}$	$r_{\vec{\omega}}$	e_u	r_u	e_p	r_p	e	$\text{eff}(\Psi)$
$E = 1, \nu = 0.25, \kappa = 1, k = 0$									
139	0.3536	2.14e+0	—	2.64e+0	—	5.51e-02	—	3.40e+0	0.249
499	0.1768	1.11e+0	0.95	1.40e+0	0.92	2.91e-02	0.92	1.79e+0	0.248
1891	0.0884	5.61e-01	0.99	7.07e-01	0.98	1.50e-02	0.96	9.02e-01	0.246
7363	0.0442	2.81e-01	1.00	3.54e-01	1.00	7.57e-03	0.98	4.52e-01	0.245
29059	0.0221	1.40e-01	1.00	1.77e-01	1.00	3.80e-03	0.99	2.26e-01	0.244
115459	0.0110	7.02e-02	1.00	8.85e-02	1.00	1.90e-03	1.00	1.13e-01	0.244
$E = 1, \nu = 0.25, \kappa = 1, k = 1$									
435	0.3536	5.33e-01	—	7.65e-01	—	7.19e-03	—	9.32e-01	0.146
1635	0.1768	1.43e-01	1.90	2.09e-01	1.87	1.96e-03	1.88	2.53e-01	0.151
6339	0.0884	3.67e-02	1.96	5.17e-02	2.02	5.11e-04	1.94	6.34e-02	0.148
24963	0.0442	9.24e-03	1.99	1.28e-02	2.02	1.30e-04	1.97	1.58e-02	0.146
99075	0.0221	2.32e-03	2.00	3.18e-03	2.01	3.29e-05	1.99	3.93e-03	0.146
394755	0.0110	5.79e-04	2.00	7.93e-04	2.00	8.26e-06	1.99	9.82e-04	0.146
$E = 10^5, \nu = 0.499, \kappa = 1, k = 0$									
139	0.3536	6.43e+2	—	7.24e+2	—	5.10e-02	—	9.68e+2	0.222
499	0.1768	3.19e+2	1.01	4.02e+2	0.85	2.85e-02	0.84	5.14e+2	0.247
1891	0.0884	1.61e+2	0.99	2.04e+2	0.98	1.49e-02	0.94	2.60e+2	0.245
7363	0.0442	8.08e+1	1.00	1.02e+2	1.00	7.55e-03	0.98	1.30e+2	0.244
29059	0.0221	4.04e+1	1.00	5.11e+1	1.00	3.80e-03	0.99	6.51e+1	0.244
115459	0.0110	2.02e+1	1.00	2.55e+1	1.00	1.90e-03	1.00	3.26e+1	0.244
$E = 10^5, \nu = 0.499, \kappa = 1, k = 1$									
435	0.3536	2.37e+2	—	4.18e+2	—	7.16e-03	—	4.81e+2	0.172
1635	0.1768	4.14e+1	2.52	5.94e+1	2.82	1.96e-03	1.87	7.24e+1	0.150
6339	0.0884	1.06e+1	1.97	1.49e+1	1.99	5.11e-04	1.94	1.83e+1	0.148
24963	0.0442	2.67e+0	1.99	3.68e+0	2.02	1.30e-04	1.97	4.55e+0	0.146
99075	0.0221	6.68e-01	2.00	9.17e-01	2.01	3.29e-05	1.99	1.13e+0	0.146
394755	0.0110	1.67e-01	2.00	2.29e-01	2.00	8.26e-06	1.99	2.83e-01	0.145
$E = 10^5, \nu = 0.499, \kappa = 10^{-12}, k = 0$									
139	0.3536	6.43e+2	—	7.24e+2	—	1.81e-03	—	9.68e+2	0.222
499	0.1768	3.19e+2	1.01	4.02e+2	0.85	4.62e-04	1.97	5.14e+2	0.247
1891	0.0884	1.61e+2	0.99	2.04e+2	0.98	1.18e-04	1.96	2.60e+2	0.245
7363	0.0442	8.08e+1	1.00	1.02e+2	1.00	3.02e-05	1.97	1.30e+2	0.244
29059	0.0221	4.04e+1	1.00	5.11e+1	1.00	7.72e-06	1.97	6.51e+1	0.244
115459	0.0110	2.02e+1	1.00	2.55e+1	1.00	2.00e-06	1.95	3.26e+1	0.244
$E = 10^5, \nu = 0.499, \kappa = 10^{-12}, k = 1$									
435	0.3536	2.37e+2	—	4.18e+2	—	9.97e-04	—	4.81e+2	0.172
1635	0.1768	4.14e+1	2.52	5.94e+1	2.82	3.60e-05	4.79	7.24e+1	0.150
6339	0.0884	1.06e+1	1.97	1.49e+1	1.99	5.40e-06	2.74	1.83e+1	0.148
24963	0.0442	2.67e+0	1.99	3.68e+0	2.02	1.15e-06	2.23	4.55e+0	0.146
99075	0.0221	6.68e-01	2.00	9.17e-01	2.01	2.73e-07	2.08	1.13e+0	0.146
394755	0.0110	1.67e-01	2.00	2.29e-01	2.00	6.69e-08	2.03	2.83e-01	0.145

rates under uniform refinement, we use the following modification to (5.1):

$$r_{(\cdot)} = -2 \log(e_{(\cdot)}/\tilde{e}_{(\cdot)}) [\log(\text{DoF}/\widetilde{\text{DoF}})]^{-1}.$$

The second example again investigates the accuracy of the three numerical methods but this time we use the L-shaped domain $\Omega = (-1, 1)^2 \setminus (0, 1)^2$ and the transmission problem has the interface defined as the segment going from the re-entrant corner $(0, 0)$ to the bottom-left corner of the domain $(-1, -1)$, and the porous domain is the one above the interface. In addition to the singularity of the geometry, we use

TABLE 5.3

Example 1C: Errors, convergence rates, and effectivity indexes under uniform mesh refinement. Smooth manufactured solutions for the rotation-based interfacial elasticity/poroelasticity problem with $k = 0, 1$.

DoFs	\mathbf{e}_{ω^P}	\mathbf{r}_{ω^P}	\mathbf{e}_{ϕ^P}	\mathbf{r}_{ϕ^P}	\mathbf{e}_{p^P}	\mathbf{r}_{p^P}	\mathbf{e}_u	\mathbf{r}_u	$\mathbf{e}_{\omega E}$	$\mathbf{r}_{\omega E}$	$\mathbf{e}_{p E}$	$\mathbf{r}_{p E}$	\mathbf{e}	$\text{eff}(\Xi)$
$E^E = E^P = 1, \nu^E = 0.25, \nu^P = 0.25, \kappa = 1, k = 0$														
139	1.5258	—	0.1982	—	3.28e-02	0.00	2.6433	—	1.48e+0	—	1.86e-01	—	3.4036	0.281
499	0.7902	0.95	0.0833	1.25	1.33e-02	1.30	1.3992	0.92	7.73e-01	0.94	8.41e-02	1.14	1.7870	0.294
1891	0.3984	0.99	0.0365	1.19	6.37e-03	1.07	0.7071	0.98	3.91e-01	0.98	3.82e-02	1.14	0.9023	0.298
7363	0.1995	1.00	0.0170	1.10	3.20e-03	0.99	0.3541	1.00	1.96e-01	1.00	1.77e-02	1.11	0.4519	0.298
29059	0.0998	1.00	0.0082	1.05	1.60e-03	1.00	0.1771	1.00	9.80e-02	1.00	8.48e-03	1.07	0.2260	0.298
115459	0.0499	1.00	0.0040	1.02	8.01e-04	1.00	0.0885	1.00	4.90e-02	1.00	4.15e-03	1.03	0.1130	0.298
$E^E = E^P = 1, \nu^E = 0.25, \nu^P = 0.25, \kappa = 1, k = 1$														
435	0.3750	—	0.0334	—	3.90e-03	—	0.7644	—	3.75e-01	—	3.62e-02	—	0.9317	0.151
1635	0.1009	1.89	0.0073	2.20	1.08e-03	1.86	0.2092	1.87	1.01e-01	1.90	7.92e-03	2.19	0.2534	0.154
6339	0.0259	1.96	0.0018	2.05	2.83e-04	1.93	0.0517	2.02	2.58e-02	1.96	1.90e-03	2.06	0.0634	0.150
24963	0.0065	1.99	0.0004	2.02	7.25e-05	1.96	0.0128	2.02	6.51e-03	1.99	4.68e-04	2.02	0.0158	0.148
99075	0.0016	2.00	0.0001	2.01	1.83e-05	1.98	0.0032	2.01	1.63e-03	2.00	1.16e-04	2.01	0.0039	0.148
394755	0.0004	2.00	2.48e-05	2.01	4.62e-06	1.99	0.0008	2.00	4.08e-04	2.00	2.90e-05	2.00	0.0010	0.147
$E^E = 10^5, E^P = 10^5, \nu^E = 0.499, \nu^P = 0.499, \kappa = 1, k = 0$														
139	450.02	—	66.730	—	2.14e-02	—	723.84	—	4.50e+2	—	6.67e+1	—	968.45	0.241
499	225.32	1.00	13.844	2.27	1.19e-02	0.85	402.24	0.85	2.25e+2	1.00	1.38e+1	2.27	513.55	0.293
1891	113.83	0.99	6.1821	1.16	6.24e-03	0.93	203.74	0.98	1.14e+2	0.99	6.18e+0	1.16	259.81	0.296
7363	57.065	1.00	2.8910	1.10	3.18e-03	0.97	102.12	1.00	5.71e+1	1.00	2.89e+0	1.10	130.22	0.297
29059	28.551	1.00	1.4069	1.04	1.60e-03	0.99	51.085	1.00	2.86e+1	1.00	1.41e+0	1.04	65.145	0.297
115459	14.277	1.00	0.6965	1.01	8.01e-04	1.00	25.543	1.00	1.43e+1	1.00	6.97e-01	1.01	32.575	0.297
$E^E = 10^5, E^P = 10^5, \nu^E = 0.499, \nu^P = 0.499, \kappa = 1, k = 1$														
435	143.37	—	87.195	—	3.85e-03	—	418.47	—	1.43e+2	—	8.72e+1	—	481.08	0.175
1635	29.208	2.30	2.0812	5.39	1.07e-03	1.84	59.380	2.82	2.92e+1	2.30	2.08e+0	5.39	72.394	0.153
6339	7.4723	1.97	0.3699	2.49	2.83e-04	1.93	14.911	1.99	7.47e+0	1.97	3.70e-01	2.49	18.283	0.150
24963	1.8825	1.99	0.0907	2.03	7.25e-05	1.96	3.6848	2.02	1.88e+0	1.99	9.07e-02	2.03	4.5477	0.148
99075	0.4716	2.00	0.0224	2.02	1.83e-05	1.98	0.9172	2.01	4.72e-01	2.00	2.24e-02	2.02	1.1345	0.148
394755	0.1180	2.00	0.0056	2.01	4.62e-06	1.99	0.2290	2.00	1.18e-01	2.00	5.57e-03	2.01	0.2834	0.147
$E^E = 10^5, E^P = 10^5, \nu^E = 0.499, \nu^P = 0.499, \kappa = 10^{-12}, k = 0$														
139	450.02	—	66.730	—	8.47e-04	—	723.84	—	4.50e+2	—	6.67e+1	—	968.45	0.241
499	225.32	1.00	13.844	2.27	2.15e-04	1.98	402.24	0.85	2.25e+2	1.00	1.38e+1	2.27	513.55	0.293
1891	113.83	0.99	6.1821	1.16	5.59e-05	1.94	203.74	0.98	1.14e+2	0.99	6.18e+0	1.16	259.81	0.296
7363	57.065	1.00	2.8910	1.10	1.45e-05	1.95	102.12	1.00	5.71e+1	1.00	2.89e+0	1.10	130.22	0.297
29059	28.551	1.00	1.4069	1.04	3.79e-06	1.93	51.085	1.00	2.86e+1	1.00	1.41e+0	1.04	65.145	0.297
115459	14.277	1.00	0.6965	1.01	1.02e-06	1.90	25.543	1.00	1.43e+1	1.00	6.97e-01	1.01	32.575	0.297
$E^E = 10^5, E^P = 10^5, \nu^E = 0.499, \nu^P = 0.499, \kappa = 10^{-12}, k = 1$														
435	143.37	—	87.195	—	6.56e-04	—	418.47	—	1.43e+2	—	8.72e+1	—	481.08	0.175
1635	29.208	2.30	2.0812	5.39	2.18e-05	4.91	59.380	2.82	2.92e+1	2.30	2.08e+0	5.39	72.394	0.153
6339	7.4723	1.97	0.3699	2.49	3.41e-06	2.68	14.911	1.99	7.47e+0	1.97	3.70e-01	2.49	18.283	0.150
24963	1.8825	1.99	0.0907	2.03	7.81e-07	2.12	3.6848	2.02	1.88e+0	1.99	9.07e-02	2.03	4.5477	0.148
99075	0.4716	2.00	0.0224	2.02	1.90e-07	2.04	0.9172	2.01	4.72e-01	2.00	2.24e-02	2.02	1.1345	0.148
394755	0.1180	2.00	0.0056	2.01	4.71e-08	2.01	0.2290	2.00	1.18e-01	2.00	5.57e-03	2.01	0.2834	0.147

TABLE 5.4

Example 2: Errors, convergence rates, and effectivity indexes under uniform versus adaptive mesh refinement for the rotation-based interfacial elasticity/poroelasticity problem on the L-shaped domain, with $k = 1$.

DoFs	$\mathbf{e}_{\omega P}$	$\mathbf{r}_{\omega P}$	$\mathbf{e}_{\phi P}$	$\mathbf{r}_{\phi P}$	$\mathbf{e}_{p P}$	$\mathbf{r}_{p P}$	\mathbf{e}_u	\mathbf{r}_u	$\mathbf{e}_{\omega E}$	$\mathbf{r}_{\omega E}$	$\mathbf{e}_{p E}$	$\mathbf{r}_{p E}$	\mathbf{e}	$\text{eff}(\Xi)$
With uniform mesh refinement														
157	8.56e-01	—	7.86e+0	—	1.36e+0	—	1.61e+0	—	9.86e-01	—	2.35e+0	—	8.246	0.071
575	3.80e-01	1.17	3.05e+0	1.37	3.64e-01	1.90	7.07e-01	1.19	4.15e-01	1.25	1.16e+0	1.02	4.199	0.151
2203	2.22e-01	0.77	1.74e+0	0.81	1.77e-01	1.05	3.92e-01	0.85	2.22e-01	0.90	6.19e-01	0.91	1.823	0.087
8627	7.72e-02	1.52	4.39e-01	1.99	4.10e-02	2.11	1.14e-01	1.78	5.98e-02	1.89	1.54e-01	2.01	0.765	0.091
34147	2.66e-02	1.54	1.09e-01	2.01	1.09e-02	1.92	3.45e-02	1.72	1.58e-02	1.92	4.10e-02	1.91	0.319	0.034
135875	1.97e-02	0.44	3.79e-02	1.53	3.64e-03	1.58	2.16e-02	0.68	7.28e-03	1.12	1.37e-02	1.58	0.248	0.152
With adaptive mesh refinement														
157	8.57e-01	—	7.86e+0	—	1.36e+0	—	1.62e+0	—	9.87e-01	0.00	2.36e+0	—	8.239	0.081
551	3.79e-01	1.30	3.05e+0	1.51	3.65e-01	2.10	7.07e-01	1.32	4.17e-01	1.37	1.16e+0	1.13	3.201	0.081
1020	2.21e-01	1.75	1.74e+0	1.82	1.77e-01	2.36	3.91e-01	1.92	2.22e-01	2.04	6.18e-01	2.05	1.822	0.087
2307	7.36e-02	2.69	4.38e-01	3.34	4.20e-02	3.52	1.11e-01	3.09	5.90e-02	3.25	1.53e-01	3.43	0.463	0.091
5779	1.81e-02	3.06	1.06e-01	3.10	1.21e-02	2.71	2.74e-02	3.04	1.45e-02	3.06	3.96e-02	2.94	0.112	0.089
20209	4.59e-03	2.19	2.67e-02	2.20	3.21e-03	2.12	6.94e-03	2.19	3.63e-03	2.21	1.02e-02	2.18	0.028	0.089
70299	1.15e-03	2.22	6.69e-03	2.22	1.23e-03	1.54	1.74e-03	2.22	9.07e-04	2.22	2.56e-03	2.21	0.007	0.090

manufactured solutions with sharp gradients near the re-entrant corner

$$p^P(x, y) = \exp(-25(x^2 + y^2)), \quad u(x, y) = (\exp(-50(x^2 + y^2)), \exp(-50(x^2 + y^2)))^t.$$

It is expected that the convergence of the methods is hindered due to the lack of regularity of the exact solutions whenever one follows a uniform mesh refinement.

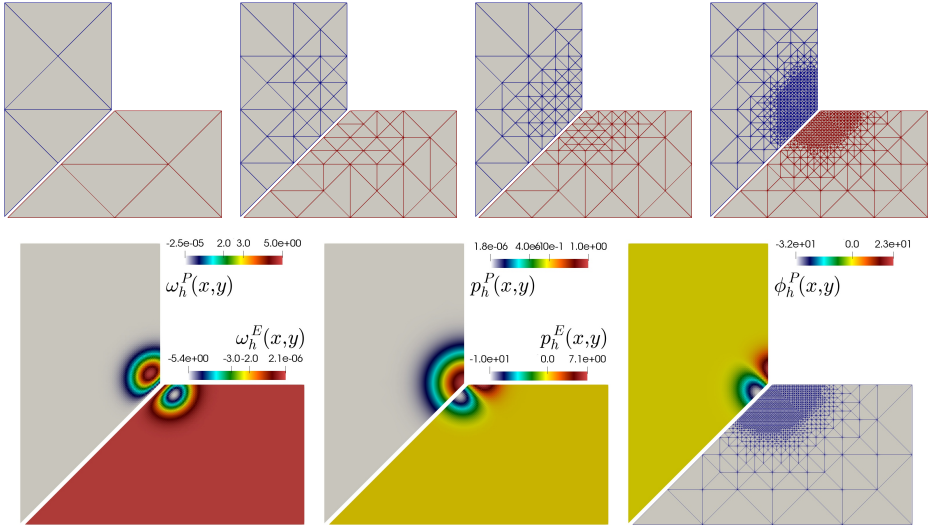


FIG. 5.1. Example 2. Adaptively refined meshes (top) and approximate solutions (bottom) for the Biot/elasticity problem.

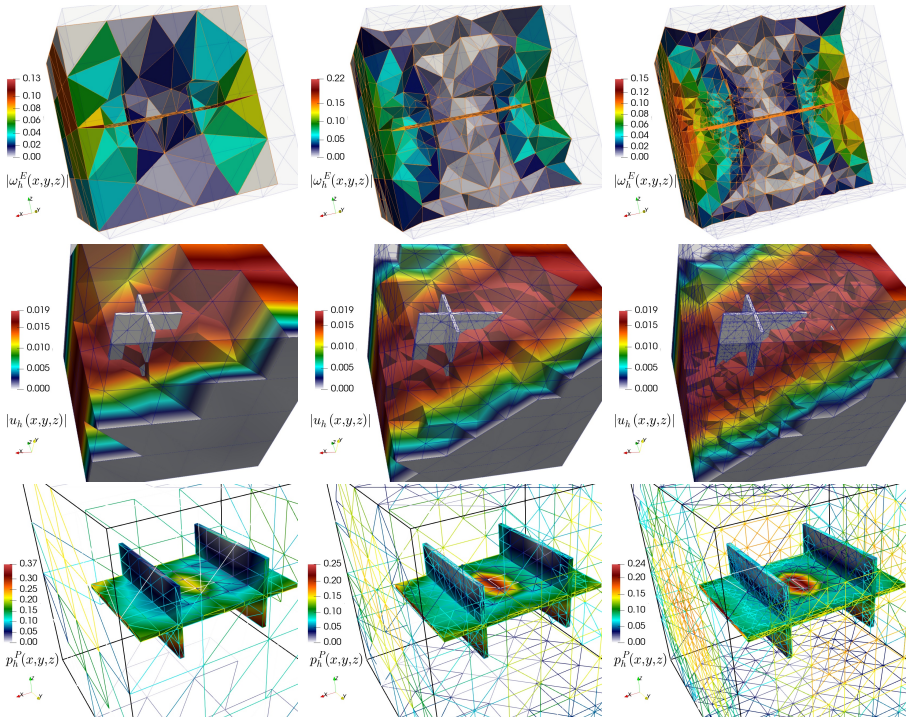


FIG. 5.2. Example 3. Approximate elastic rotation on a horizontally clipped elastic geometry (top), displacement on a diagonally clipped domain (center), and fluid pressure on a zoomed poroelastic domain (bottom), for three steps of adaptive refinement for the Biot/elasticity application in fractured reservoirs.

Such a slower error decay is clearly observed in the top half of Table 5.4, while adaptive mesh refinement (with a Dörfler constant of $\zeta = 0.001$) yields asymptotic optimal convergence evidenced on the bottom half of the table, where also one reaches much smaller errors using a fraction of the degrees of freedom needed in the uniform case. Here we focus on the methods with $k = 1$, and samples of adaptively refined meshes and approximate solutions are portrayed in Figure 5.1. In this case we have used the following contrast of parameters between the subdomains: $c_0 = 0$, $\alpha = 1$, $E^E = 10$, $E^P = 1$, $\nu^E = 0.25$, $\nu^P = 0.45$, $\xi = 1$, $\kappa = 10^{-3}$.

The last test illustrates the use of mesh adaptivity guided by the a posteriori error estimator Ξ on an interface elasticity/poroelasticity problem applied to oil reservoir poromechanics, similarly to the test in [24, sect. 8.2] (see also [26, 4]). In CO₂ sequestration in deep subsurface reservoirs one is interested in the distribution of pressure and displacement across the interface between the nonpay rock and the aquifer zones in the case where the poroelastic domain is an array of thin-walled structures fully surrounded by an elastic region. The multidomain is the unit cube $\Omega = (0, 1)^3 \text{ m}^3$ and the aquifer array has a width of 0.015 m. A well is represented by a localized source $s^P(x, y, z) = s_0 \exp(-1000[(x - 0.5)^2 + (y - 0.5)^2 + (z - 0.5)^2])$. This is an injection zone of relatively small radius reaching the center of the pay zone at (0.5, 0.5, 0.5). On the surface of the nonpay rock we impose the sliding condition $\mathbf{u} \cdot \mathbf{n} = 0$. The interfacial conditions are as in (4.1i). The simulation uses the following values for the model parameters: “ $s_0 = 0.5$, $c_0 = 10^{-3}$, $\alpha = 0.75$, $E^E = 5 \cdot 10^3$, $E^P = 10^3$, $\nu^E = 0.3$, $\nu^P = 0.45$, $\xi = 10^{-3}$, $\kappa = 10^{-7}$, $\mathbf{g} = (0, 0, -9.81)^t$.”

Initial coarse meshes are constructed for both subdomains, then we solve the coupled transmission problem, and then apply six steps of the iterative mesh refinement strategy based on the estimator Ξ . To observe how the adaptivity takes place on both elastic and poroelastic domains, we plot in Figure 5.2 samples of the approximate solutions on the first three steps of adaptive mesh refinement. The concentration of the amount of fluid near the center of the pay zone is seen in the first row, and we can also see the concentration of refinement near the interface in all panels.

6. Concluding remarks. In this paper we have developed the a posteriori error analysis for the interfacial coupling between an elastic solid and a poroelastic material. The formulation is written using rotations as part of the unknowns in both subdomains. We establish reliability and efficiency of three different models, and present a series of computational results confirming the theoretical properties of the a posteriori error estimators.

Extensions of this work include H(div)-conforming discretizations, the coupling with advection-diffusion-reaction systems following [40], and the case of nonlinear permeability (depending on the total amount of fluid or only on the displacement divergence) as used in, e.g., [13, 15] and [3, 17]. Nonlinear extensions including Forchheimer-type terms, as in, e.g., [14], or with the theory from [22] are also feasible. A much more challenging problem is the interface coupling in the large-deformation regime, which could follow the recent theory in [9, 10], so far only available for linearised poro-hyperelasticity.

Appendix A. Well-posedness analysis for rotation-based poroelasticity.

The bilinear forms and the linear functionals appearing in the variational problem of interest (cf. section 3) are all bounded by constants independent of μ^P and λ^P [4, 5]. In addition, we have the following result.

LEMMA A.1. *Let $(\vec{\omega}, \mathbf{u}, p) \in \mathbf{H} \times \mathbf{V} \times Q$, where $\vec{\omega} = (\boldsymbol{\omega}, \phi)$, be a solution of the*

system (3.3a)–(3.3c); then there exists a constant $C > 0$, such that

$$(A.1) \quad \|(\mathbf{u}, \boldsymbol{\omega}, \phi, p)\| \leq C\{(\mu^P)^{-1/2}\|\mathbf{f}^P\|_{0,\Omega} + \|(\kappa/\xi)^{1/2}\rho\mathbf{g}\|_{0,\Omega} + \rho_1^{1/2}\|s^P\|_{0,\Omega}\},$$

where $\rho_1 = \min((c_0 + \frac{\alpha^2}{(2\mu^P + \lambda^P)})^{-1}, (\kappa/\xi)^{-1})$.

Proof. Using Theorem 3.1 implies

$$C_2 \|(\mathbf{u}, \boldsymbol{\omega}, \phi, p)\|^2 \leq B_P((\mathbf{u}, \boldsymbol{\omega}, \phi, p), (\mathbf{v}, \boldsymbol{\theta}, \psi, q)) = F(\mathbf{v}) + G(q),$$

with $\|(\mathbf{v}, \boldsymbol{\theta}, \psi, q)\| \leq C_1 \|(\mathbf{u}, \boldsymbol{\omega}, \phi, p)\|$, where C_1 and C_2 are constants given in Theorem 3.1. And (A.1) results from applying the Cauchy–Schwarz inequality. \square

A.1. Solvability of the continuous problem. Let us rewrite (3.3a)–(3.3c) as follows: find $\vec{\mathbf{u}} := (\vec{\boldsymbol{\omega}}, \mathbf{u}, p) \in \mathbf{X} := \mathbf{H} \times \mathbf{V} \times Q$ such that $(\mathcal{S} + \mathcal{T})\vec{\mathbf{u}} = \mathcal{F}$, where the linear operators $\mathcal{S} : \mathbf{X} \rightarrow \mathbf{X}^*$, $\mathcal{T} : \mathbf{X} \rightarrow \mathbf{X}^*$, and $\mathcal{F} \in \mathbf{X}^*$ are defined as

$$\begin{aligned} \langle \mathcal{S}(\vec{\mathbf{u}}), \vec{\mathbf{v}} \rangle &:= a(\vec{\boldsymbol{\omega}}, \vec{\boldsymbol{\theta}}) + b_1(\vec{\boldsymbol{\theta}}, \mathbf{u}) - b_1(\vec{\boldsymbol{\omega}}, \mathbf{v}) + c(p, q), \\ \langle \mathcal{T}(\vec{\mathbf{u}}), \vec{\mathbf{v}} \rangle &:= -b_2(\vec{\boldsymbol{\theta}}, p) - b_2(\vec{\boldsymbol{\omega}}, q), \quad \langle \mathcal{F}, \vec{\mathbf{v}} \rangle := -F(\mathbf{v}) - G(q) \end{aligned}$$

for all $\vec{\mathbf{u}} := (\vec{\boldsymbol{\omega}}, \mathbf{u}, p)$, $\vec{\mathbf{v}} := (\vec{\boldsymbol{\theta}}, \mathbf{v}, q) \in \mathbf{X}$, where $\langle \cdot, \cdot \rangle$ is the duality pairing between \mathbf{X} and its dual \mathbf{X}^* .

LEMMA A.2. *The operator $\mathcal{S} : \mathbf{X} \rightarrow \mathbf{X}^*$ is invertible.*

Proof. First, for a given functional $\mathcal{F} := (\mathcal{F}_{\mathbf{H}}, \mathcal{F}_{\mathbf{V}}, \mathcal{F}_Q)$, observe that establishing the invertibility of \mathcal{S} is equivalent to proving the unique solvability of the operator problem

$$(A.2) \quad \mathcal{S}(\vec{\mathbf{u}}) = \mathcal{F}.$$

Furthermore, proving unique solvability of (A.2) is in turn equivalent to proving the unique solvability of the two following uncoupled problems: find $(\vec{\boldsymbol{\omega}}, \mathbf{u}) \in \mathbf{H} \times \mathbf{V}$ such that

$$(A.3) \quad \begin{aligned} a(\vec{\boldsymbol{\omega}}, \vec{\boldsymbol{\theta}}) + b_1(\vec{\boldsymbol{\theta}}, \mathbf{u}) &= F_{\mathbf{H}}(\vec{\boldsymbol{\theta}}) & \forall \vec{\boldsymbol{\theta}} \in \mathbf{H}, \\ b_1(\vec{\boldsymbol{\omega}}, \mathbf{v}) &= F_{\mathbf{V}}(\mathbf{v}) & \forall \mathbf{v} \in \mathbf{V}, \end{aligned}$$

and find $p \in Q$, such that

$$(A.4) \quad c(p, q) = F_Q(q) \quad \forall q \in Q,$$

where $F_{\mathbf{H}}$, $F_{\mathbf{V}}$, and F_Q are the functionals induced by $\mathcal{F}_{\mathbf{H}}$, $\mathcal{F}_{\mathbf{V}}$, and \mathcal{F}_Q , respectively. The unique solvability of (A.4) follows by virtue of the Lax–Milgram lemma, and the well-posedness of (A.3) follows from a straightforward application of the Babuška–Brezzi theory. \square

LEMMA A.3. *The operator $\mathcal{T} : \mathbf{X} \rightarrow \mathbf{X}^*$ is compact.*

Proof. We begin by defining the operator $\mathbb{B} : L^2(\Omega) \rightarrow Q$ as

$$\langle \mathbb{B}(\psi), q \rangle_{0,\Omega} := \alpha(2\mu^P + \lambda^P)^{-1} \int_{\Omega} q\psi \quad \forall q \in Q, \forall \psi \in L^2(\Omega).$$

This operator is the composition of a compact injection and a continuous map and it is therefore compact. And denoting by \mathbb{B}^* the adjoint of \mathbb{B} , we infer that the following map is also compact:

$$\mathcal{T}(\vec{\mathbf{u}}) = ((\mathbf{0}, -\mathbb{B}(\phi), \mathbf{0}, 0), \mathbf{0}, -\mathbb{B}^*(p)).$$

\square

LEMMA A.4. *The operator $(\mathcal{S} + \mathcal{T}) : \mathbf{X} \rightarrow \mathbf{X}^*$ is injective.*

Proof. It is sufficient to show that the only solution to the homogeneous problem

$$\begin{aligned} a(\vec{\omega}, \vec{\theta}) + b_1(\vec{\theta}, \mathbf{u}) - b_2(\vec{\theta}, p) &= 0 & \forall \vec{\theta} \in \mathbf{H}, \\ b_1(\vec{\omega}, \mathbf{v}) &= 0 & \forall \mathbf{v} \in \mathbf{V}, \\ b_2(\vec{\omega}, q) - c(p, q) &= 0 & \forall q \in Q \end{aligned}$$

is the null-vector in \mathbf{X} . Thus, from Lemma A.1, and the fact that $F = G = 0$, we have $\mathbf{u} = \mathbf{0}$, $\vec{\omega} = \mathbf{0}$, $p = 0$. \square

By virtue of Lemmas A.1, A.2, A.3, and A.4, and the abstract Fredholm alternative theorem, one straightforwardly derives the main result of this section, stated in the upcoming theorem.

THEOREM A.1. *There exists a unique solution $(\vec{\omega}, \mathbf{u}, p) \in \mathbf{H} \times \mathbf{V} \times Q$, where $\vec{\omega} = (\omega, \phi)$, to (3.3a)–(3.3c). Furthermore, there exists a positive constant $C > 0$, such that*

$$\|(\mathbf{u}, \omega, \phi, p)\| \leq C \{ (\mu^P)^{-1/2} \|f^P\|_{0,\Omega} + \|(\kappa/\xi)^{1/2} \rho g\|_{0,\Omega} + \rho_1^{1/2} \|s^P\|_{0,\Omega} \},$$

where $\rho_1 = \min((c_0 + \frac{\alpha^2}{(2\mu^P + \lambda^P)})^{-1}, (\kappa/\xi)^{-1})$.

Appendix B. A priori error analysis for rotation-based poroelasticity.

Denoting $\mathbf{W}_h \times Z_h := \mathbf{H}_h$, a Galerkin scheme for (3.3a)–(3.3c) is as follows: find $(\vec{\omega}_h, \mathbf{u}_h, p_h) := ((\omega_h, \phi_h), \mathbf{u}_h, p_h) \in \mathbf{H}_h \times \mathbf{V}_h \times Q_h$ such that

$$\begin{aligned} (B.1) \quad a(\vec{\omega}_h, \vec{\theta}_h) + b_1(\vec{\theta}_h, \mathbf{u}_h) - b_2(\vec{\theta}_h, p_h) &= 0 & \forall \vec{\theta}_h := (\theta_h, \psi_h) \in \mathbf{H}_h, \\ (B.2) \quad b_1(\vec{\omega}_h, \mathbf{v}_h) &= F(\mathbf{v}_h) & \forall \mathbf{v}_h \in \mathbf{V}_h, \\ (B.3) \quad b_3(\vec{\omega}_h, q_h) - c(p_h, q_h) &= G(q_h) & \forall q_h \in Q_h. \end{aligned}$$

B.1. Stability of the discrete problem. All bilinear forms and functionals introduced in section 3 preserve stability on the discrete spaces. Also, $a(\cdot, \cdot)$, and $c(\cdot, \cdot)$ maintain coercivity on \mathbf{H}_h and Q_h , respectively. Such stability properties permit us to establish the well-posedness of (B.1)–(B.3).

THEOREM B.1. *There exists a unique solution $(\vec{\omega}_h, \mathbf{u}_h, p_h) \in \mathbf{H}_h \times \mathbf{V}_h \times Q_h$, where $\vec{\omega}_h = (\omega_h, \phi_h)$, to (B.1)–(B.3). Furthermore, there exists a positive constant $C_{\text{Stab}} > 0$, independent of h , μ^P , λ^P , such that*

$$\|(\mathbf{u}_h, \omega_h, \phi_h, p_h)\| \leq C \{ (\mu^P)^{-1/2} \|f^P\|_{0,\Omega} + \|(\kappa/\xi)^{1/2} \rho g\|_{0,\Omega} + \rho_1^{1/2} \|s^P\|_{0,\Omega} \},$$

where $\rho_1 = \min((c_0 + \frac{\alpha^2}{(2\mu^P + \lambda^P)})^{-1}, (\kappa/\xi)^{-1})$.

Proof. The proof follows as in the proof of Lemmas A.1 and A.4. \square

B.2. A priori error bounds. Approximation properties of the spaces in (3.4) (see, e.g., [16]) produce the following theoretical rate of convergence:

$$\begin{aligned} \|(\mathbf{u} - \tilde{\mathbf{u}}, \omega - \tilde{\omega}, \phi - \tilde{\phi}, p - \tilde{p})\| &\leq C h^{\min\{s, k+1\}} (\|\omega\|_{s,\Omega} + \sqrt{\mu^P} \|\mathbf{u}\|_{s+1,\Omega} \\ &\quad + \rho_\phi \|\phi\|_{s,\Omega} + \rho_p \|p\|_{s+1,\Omega}), \end{aligned}$$

where $\rho_\phi = \sqrt{1/\mu^P} + \sqrt{1/(2\mu^P + \lambda^P)}$, $\rho_p = \max((c_0 + \frac{\alpha^2}{(2\mu^P + \lambda^P)})^{1/2}, (\kappa/\xi)^{1/2})$, and $C > 0$.

THEOREM B.2. *In addition to the hypotheses of Theorems A.1 and B.1, assume that there exists $s > 0$ such that $\omega \in \mathbf{H}^s(\Omega)$, $\mathbf{u} \in \mathbf{H}^{1+s}(\Omega)$, $\phi \in \mathbf{H}^s(\Omega)$, $p \in \mathbf{H}^{1+s}(\Omega)$. Then, there exists $C_{\text{conv}} > 0$, independent of h and λ^P , such that with the discrete spaces (3.4), there holds*

$$\begin{aligned} \|(\mathbf{u} - \mathbf{u}_h, \omega - \omega_h, \phi - \phi_h, p - p_h)\| &\leq C_{\text{conv}} h^{\min\{s, k+1\}} (\|\omega\|_{s,\Omega} + \sqrt{\mu^P} \|\mathbf{u}\|_{s+1,\Omega} \\ &\quad + \rho_\phi \|\phi\|_{s,\Omega} + \rho_p \|p\|_{s+1,\Omega}). \end{aligned}$$

Proof. Using the triangle inequality we can split the error into two parts,

$$\begin{aligned} \|(\mathbf{u} - \mathbf{u}_h, \omega - \omega_h, \phi - \phi_h, p - p_h)\| &\leq \|(\mathbf{u} - \tilde{\mathbf{u}}, \omega - \tilde{\omega}, \phi - \tilde{\phi}, p - \tilde{p})\| \\ &\quad + \|(\tilde{\mathbf{u}} - \mathbf{u}_h, \tilde{\omega} - \omega_h, \tilde{\phi} - \phi_h, \tilde{p} - p_h)\|. \end{aligned}$$

Then we can estimate the first term thanks to approximation results. To estimate the second term, we use the stability result given in Theorem 3.1; then

$$\begin{aligned} C_1 \|(\tilde{\mathbf{u}} - \mathbf{u}_h, \tilde{\omega} - \omega_h, \tilde{\phi} - \phi_h, \tilde{p} - p_h)\|^2 \\ &\leq B_P((\tilde{\mathbf{u}} - \mathbf{u}_h, \tilde{\omega} - \omega_h, \tilde{\phi} - \phi_h, \tilde{p} - p_h), (\mathbf{v}, \boldsymbol{\theta}, \psi, q)) \\ &\leq B_P((\tilde{\mathbf{u}} - \mathbf{u}, \tilde{\omega} - \omega, \tilde{\phi} - \phi, \tilde{p} - p), (\mathbf{v}, \boldsymbol{\theta}, \psi, q)), \end{aligned}$$

with $\|(\mathbf{v}, \boldsymbol{\theta}, \psi, q)\| \leq C_2 \|(\tilde{\mathbf{u}} - \mathbf{u}_h, \tilde{\omega} - \omega_h, \tilde{\phi} - \phi_h, \tilde{p} - p_h)\|$. We can then invoke the continuity results to get

$$C_1 \|(\tilde{\mathbf{u}} - \mathbf{u}_h, \tilde{\omega} - \omega_h, \tilde{\phi} - \phi_h, \tilde{p} - p_h)\| \leq C_2 \|(\tilde{\mathbf{u}} - \mathbf{u}, \tilde{\omega} - \omega, \tilde{\phi} - \phi, \tilde{p} - p)\|. \quad \square$$

REFERENCES

- [1] E. AHMED, F. A. RADU, AND J. M. NORDBOTTEL, *Adaptive poromechanics computations based on a posteriori error estimates for fully mixed formulations of Biot's consolidation model*, Comput. Methods Appl. Mech. Engrg., 347 (2019), pp. 264–294.
- [2] M. S. ALNÆS, J. BLECHTA, J. HAKE, A. JOHANSSON, B. KEHLER, A. LOGG, C. RICHARDSON, J. RING, M. E. ROGNES, AND G. N. WELLS, *The FEniCS project version 1.5*, Archive of Numerical Software, 3 (2015), pp. 9–23.
- [3] R. ALTMANN AND R. MAIER, *A decoupling and linearizing discretization for weakly coupled poroelasticity with nonlinear permeability*, SIAM J. Sci. Comput., 44 (2022), pp. B457–B478, preprint, <https://doi.org/10.1137/21M1413985>.
- [4] V. ANAYA, Z. DE WIJN, B. GÓMEZ-VARGAS, D. MORA, AND R. RUIZ-BAIER, *Rotation-based mixed formulations for an elasticity-poroelasticity interface problem*, SIAM J. Sci. Comput., 42 (2020), pp. B225–B249, <https://doi.org/10.1137/19M1268343>.
- [5] V. ANAYA, Z. DE WIJN, D. MORA, AND R. RUIZ-BAIER, *Mixed displacement-rotation-pressure formulations for linear elasticity*, Comput. Methods Appl. Mech. Engrg., 344 (2019), pp. 71–94, <https://doi.org/10.1016/j.cma.2018.09.029>.
- [6] V. ANAYA, B. GÓMEZ-VARGAS, D. MORA, AND R. RUIZ-BAIER, *Incorporating variable viscosity in vorticity-based formulations for Brinkman equations*, C. R. Math. Acad. Sci. Paris, 357 (2019), pp. 552–560.
- [7] S. ATLURI AND A. CAZZANI, *Rotations in computational solid mechanics*, Arch. Comput. Methods Engrg., 2 (1995), pp. 49–138.
- [8] F. BALLARIN, *Multiphenics – Easy Prototyping of Multiphysics Problems in FEniCS*, <https://mathlab.sissa.it/multiphenics>, accessed 2021-01-10.
- [9] N. BARNAFI, B. GÓMEZ-VARGAS, W. DE JESUS LOURENÇO, R. F. REIS, B. M. ROCHA, M. LOBOSCO, R. RUIZ-BAIER, AND R. W. DOS SANTOS, *Mixed Methods for Large-Strain Poroelasticity/Chemotaxis Models Simulating the Formation of Myocardial Oedema*, preprint, <https://arxiv.org/abs/2111.04206>, 2022.

- [10] N. BARNAFI, P. ZUNINO, L. DEDÈ, AND A. QUARTERONI, *Mathematical analysis and numerical approximation of a general linearized poro-hyperelastic model*, Comput. Math. Appl., 91 (2021), pp. 202–228.
- [11] C. BERNARDI AND N. CHORFI, *Spectral discretization of the vorticity, velocity, and pressure formulation of the Stokes problem*, SIAM J. Numer. Anal., 44 (2006), pp. 826–850, <https://doi.org/10.1137/050622687>.
- [12] F. BERTRAND AND G. STARKE, *A posteriori error estimates by weakly symmetric stress reconstruction for the Biot problem*, Comput. Math. Appl., 91 (2021), pp. 3–16.
- [13] L. BOCIU, B. MUHA, AND J. T. WEBSTER, *Weak Solutions in Nonlinear Poroelasticity with Incompressible Constituents*, preprint, <https://arxiv.org/abs/2108.10977>, 2022.
- [14] J. W. BOTH, J. M. NORDBOTTEN, AND F. A. RADU, *Free energy diminishing discretization of Darcy-Forchheimer flow in poroelastic media*, in Finite Volumes for Complex Applications IX - Methods, Theoretical Aspects, Examples, R. Klöfkorn, E. Keilegavlen, F. A. Radu, and J. Fuhrmann, eds., 2020, Springer, Cham, pp. 203–211.
- [15] M. BOTTI, D. A. DI PIETRO, AND P. SOCHALA, *A hybrid high-order discretization method for nonlinear poroelasticity*, Comput. Methods Appl. Math., 20 (2020), pp. 227–249.
- [16] F. BREZZI AND M. FORTIN, *Mixed and Hybrid Finite Element Methods*, Springer-Verlag, Berlin, 1991.
- [17] Y. CAO, S. CHEN, AND A. MEIR, *Analysis and numerical approximations of equations of nonlinear poroelasticity*, Discrete Contin. Dyn. Syst. Ser. B, 18 (2013), pp. 1253–1273.
- [18] W. DÖRFLER, *A convergent adaptive algorithm for Poisson's equation*, SIAM J. Numer. Anal., 33 (1996), pp. 1106–1124, <https://doi.org/10.1137/0733054>.
- [19] F. DUBOIS, M. SALAÜN, AND S. SALMON, *First vorticity-velocity-pressure numerical scheme for the Stokes problem*, Comput. Methods Appl. Mech. Engrg., 192 (2003), pp. 4877–4907.
- [20] E. ELISEUSSEN, M. E. ROGNES, AND T. B. THOMPSON, *A-posteriori Error Estimation and Adaptivity for Multiple-Network Poroelasticity*, preprint, <https://arxiv.org/abs/2111.13456>, 2021.
- [21] A. ERN, *Vorticity-velocity formulation of the Stokes problem with variable density and viscosity*, C. R. Acad. Sci. Paris Sér. I Math., 323 (1996), pp. 1159–1164.
- [22] A. FUMAGALLI AND F. S. PATACCINI, *Model adaptation for non-linear elliptic equations in mixed form: Existence of solutions and numerical strategies*, ESAIM Math. Model. Numer. Anal., 56 (2022), pp. 565–592.
- [23] G. N. GATICA, *A Simple Introduction to the Mixed Finite Element Method. Theory and Applications*, Springer-Verlag, Berlin, 2014.
- [24] V. GIRAUT, X. LU, AND M. F. WHEELER, *A posteriori error estimates for Biot system using Enriched Galerkin for flow*, Comput. Methods Appl. Mech. Engrg., 369 (2020), e113185, <https://doi.org/10.1016/j.cma.2020.113185>.
- [25] V. GIRAUT AND P.-A. RAVIART, *Finite Element Methods for Navier-Stokes Equations: Theory and Algorithms*, 1st ed., Springer, 1986.
- [26] V. GIRAUT, M. F. WHEELER, T. ALMANI, AND S. DANA, *A priori error estimates for a discretized poro-elastic-elastic system solved by a fixed-stress algorithm*, Oil Gas Sci. Technol., 74 (2019), 24, <https://doi.org/10.2516/ogst/2018071>.
- [27] R. GLOWINSKI AND O. PIRONNEAU, *Numerical methods for the first biharmonic equation and for the two-dimensional Stokes problem*, SIAM Rev., 21 (1979), pp. 167–212, <https://doi.org/10.1137/1021028>.
- [28] T. HUGHES AND L. FRANCA, *A new finite element formulation for CFD: VII. The Stokes problem with various well-posed boundary conditions: Symmetric formulations that converge for all velocity/pressure spaces*, Comput. Methods Appl. Mech. Engrg., 65 (1987), pp. 85–96.
- [29] A. IBRAHIMBEGOVIC, *Finite elastic deformations and finite rotations of 3d continuum with independent rotation field*, Rev. Européenne Élém. Finis, 4 (1995), pp. 555–576.
- [30] A. KHAN AND D. J. SILVESTER, *Robust a posteriori error estimation for mixed finite element approximation of linear poroelasticity*, IMA J. Numer. Anal., 41 (2021), pp. 2000–2025.
- [31] K. KUMAR, S. KYAS, J. M. NORDBOTTEN, AND S. REPIN, *Guaranteed and computable error bounds for approximations constructed by an iterative decoupling of the Biot problem*, Comput. Math. Appl., 91 (2021), pp. 122–149.
- [32] J. LEE, K. MARDAL, AND R. WINTHER, *Parameter-robust discretization and preconditioning of Biot's consolidation model*, SIAM J. Sci. Comput., 39 (2017), pp. A1–A24, <https://doi.org/10.1137/15M1029473>.
- [33] Y. LI AND L. T. ZIKATANOV, *Residual-based a posteriori error estimates of mixed methods for a three-field Biot's consolidation model*, IMA J. Numer. Anal., 42 (2022), pp. 620–648.
- [34] T. MERLINI AND M. MORANDINI, *The helicoidal modeling in computational finite elasticity*,

III: *Finite element approximation for non-polar media*, Internat. J. Solids Structures, 42 (2005), pp. 6475–6513.

- [35] J. NORDBOTSEN, T. RAHMAN, S. REPIN, AND J. VALDMAN, *A posteriori error estimates for approximate solutions of the Barenblatt-Biot poroelastic model*, Comput. Methods Appl. Math., 10 (2010), pp. 302–314.
- [36] R. OYARZÚA, S. RHEBERGEN, M. SOLANO, AND P. ZÚÑIGA, *Error analysis of a conforming and locking-free four-field formulation for the stationary Biot's model*, ESAIM Math. Model. Numer. Anal., 55 (2021), pp. S475–S506.
- [37] R. OYARZÚA AND R. RUIZ-BAIER, *Locking-free finite element methods for poroelasticity*, SIAM J. Numer. Anal., 54 (2016), pp. 2951–2973, <https://doi.org/10.1137/15M1050082>.
- [38] R. RIEDLBECK, D. A. DI PIETRO, A. ERN, S. GRANET, AND K. KAZYMYRENKO, *Stress and flux reconstruction in Biot's poro-elasticity problem with application to a posteriori error analysis*, Comput. Math. Appl., 73 (2017), pp. 1593–1610.
- [39] R. VERFÜRTH, *A posteriori error estimation techniques for finite element methods*, Oxford University Press, Oxford, 2013.
- [40] N. VERMA, B. GÓMEZ-VARGAS, L. M. DE OLIVEIRA VILACA, S. KUMAR, AND R. RUIZ-BAIER, *Well-posedness and discrete analysis for advection-diffusion-reaction in poroelastic media*, Appl. Anal., (2021), pp. 1–28.